Masterarbeits

Structure embeddings for OpenSSH heap dump analysis

A report by

Lahoche, Clément Claude Martial

Prüfer

Prof. Dr. Michael Granitzer

Christofer Fellicious

Prof. Dr. Pierre-Edouard Portier

October 18, 2023

Abstract

Acknowledgements

Contents

List of Figures

List of Tables

Algorithms and program code

1 Introduction

Digital forensics is a linchpin in cybersecurity, enabling the extraction of vital evidence from devices like PCs. This evidence is key for detecting malware and tracing intruder activities. Analyzing a device's main memory is a go-to technique in this field. The fusion of machine learning promises to amplify and streamline these analyses.

With the rising need for encrypted communication, Secure Shell (SSH) protocols are now commonplace. However, these security-focused channels can inadvertently shield malicious actions, posing challenges to standard investigative approaches. Cutting-edge research offers solutions. The work in *SmartKex: Machine Learning Assisted SSH Keys Extraction From The Heap Dump* [9] highlights how machine learning can boost the extraction of session keys from OpenSSH memory images. In a complementary vein, „SSHkex: Leveraging virtual machine introspection for extracting SSH keys and decrypting SSH network traffic“ [29] showcases the power of Virtual Machine Introspection (VMI) for direct SSH key extraction.

Inspired by *SmartKex: Machine Learning Assisted SSH Keys Extraction From The Heap Dump*, this thesis zeroes in on a central challenge: data embedding. While previous studies set the stage for key extraction, the data embedding technique, especially windowing, can be optimized. The design of data embeddings is pivotal for machine learning efficacy, especially in nuanced tasks like memory analysis. This research introduces fresh embedding strategies, aiming to refine extraction and unearth deeper memory snapshot patterns. Merging graph embeddings with advanced machine learning, the goal is to craft a sophisticated toolkit for OpenSSH heap dump studies, bridging digital forensics and machine learning.

2 Research Questions

- What are the most effective techniques for embedding byte sequences, especially when aiming to extract structures containing SSH keys for machine learning purposes?
- Do the embeddings designed show noticeable differences based on the various applications of OpenSSH, considering the wide range of SSH key sizes and the complex operations of OpenSSH?
- How can we ensure the consistency and stability of these embeddings across the wide variety of OpenSSH versions and usages?

3 Structure of the Thesis

Explain the structure of the thesis.

4 Related work

The embedding of memory heap dumps for the detection of SSH keys is a niche yet crucial area of research, especially in the context of cybersecurity and digital forensics. This section reviews two seminal papers that have significantly influenced our work: *SSHKex*, which delves into Virtual Machine Introspection (VMI) and memory forensics, and *SmartKex*, which employs machine learning techniques for SSH key detection.

4.1 Virtual Machine Introspection and Memory Forensics: SSHKex

SSHKex is an initiative that delves into the intricacies of analyzing encrypted SSH traffic. By harnessing the capabilities of VMI, Sentanoe and Reiser spearheaded this project to discreetly extract SSH keys and decrypt SSH network communications, ensuring the preservation of evidence [29].

The methodology adopted by **SSHKex** seamlessly integrates conventional network traffic monitoring with dynamic SSH session key retrieval. A pivotal assumption is the familiarity with the SSH server's implementation, which is vital for the extraction process. Tools such as LibVMI and Volatility, under the VMI umbrella, are employed to provide an unaltered perspective of the guest VM's state, enabling the efficient pinpointing of SSH session keys within a Linux system's primary memory.

Outlined below is the **SSHKex** key extraction procedure:

1. **Data Structure Insights**: The technique capitalizes on in-depth understanding of the data structures housing the keys. Debugging symbols, tailored to the SSH version on the target, offer crucial offset values, aiding in key material extraction. Key structures encompass `struct ssh`, `struct session_state`, `struct newkeys`, and `struct sshenc`, which collectively house details like IP addresses, session statuses, and encryption keys.

2. **OpenSSH Function Tracing**: This step involves tracing functions to accurately locate data structures and timely key extraction. Emphasis is on `kex_derive_keys` (for key generation initiation) and `do_authentication2` (triggering user authentication).

3. **Breakpoint Implementation**: For debugging purposes, software breakpoints are strategically embedded in the program's execution. Using VMI, SSHKex introduces these breakpoints at the starting points of the two pivotal functions mentioned above.

4. **Extraction of Keys**: The `kex_derive_keys` function's invocation prompts SSHKex to initially capture the `ssh struct`'s address. The subsequent call to the `do_authentication2` function facilitates the extraction of actual keys, adhering to recognized structures.

5. **Key Classification**: OpenSSH designates distinct indices in the `newkeys` structure for client-to-server and vice versa keys. SSHKex's extraction is based on these specific indices.

6. **Managing Multiple Sessions**: OpenSSH handles numerous SSH sessions by initiating child processes. SSHKex broadens its extraction approach to each child process, identifying them via their distinct process IDs.

A standout feature of **SSHKex** is its commitment to discretion, conservation, and maintaining evidence authenticity. The methodology is crafted to minimize intrusiveness, ensuring no alterations to the scrutinized system. This is paramount in forensic scenarios where evidence sanctity is of utmost importance.

4.2 Machine Learning for SSH Key Detection: SmartKex

SmartKex builds upon the foundation of extracting SSH keys from heap memory dumps, aiming to streamline and automate the process. The project stands out by integrating machine learning techniques, enhancing the efficiency and precision of key extraction. This contrasts with the more complex SSHKex approach, which necessitates in-depth SSH knowledge and breakpoint injections.

SmartKex proposes two key extraction methods:

- *Brute-Force Baseline Method*: A conventional method that sifts through heap memory, identifying potential keys based on recognized patterns.
- *Machine Learning-Assisted Method*: Utilizes a Random Forest algorithm, trained on an imbalanced dataset balanced using SMOTE. While this method offers high precision and recall, it's probabilistic, making it less exact than the brute-force approach.

4.2.1 Baseline Brute-Force Method

The brute-force approach of **SmartKex** encompasses the following steps [9]:

1. *Heap Dump Creation*: Binary files of the OpenSSH server process are generated (methodology unspecified in SmartKex) and are presumed to be based on a linux-x86_64 architecture.
2. *Data Trimming*: The method trims irrelevant memory pages based on Hamming distance to reduce heap size.
3. *Key Search*: The algorithm scans the heap, considering a 128-byte length as a potential key, iterating until the heap's end.
4. *Decryption Trials*: Each potential key undergoes decryption attempts on network packets. Failed attempts lead to the next potential key.

Despite its exactness, the brute-force method is resource-intensive and is less efficient when keys are towards the heap dump's end.

4.2.2 Machine Learning-Assisted Method

SmartKex's innovation lies in its machine learning methodology, which, while sacrificing exactness, offers speed and accuracy. The method also reduces the heap to under 2% of its original size. The steps include:

1. *Heap Dump Inputs*: As with the brute-force method, binary files from OpenSSH are the primary inputs.
2. *Data Preprocessing*: The heap dump is reshaped into an N $\times$ 8 matrix. High entropy sections, potential encryption keys, are flagged using logical operations on byte differences.
3. *Model Training*: A Random Forest algorithm is trained on 128-byte segments of the processed heap. Given the dataset's imbalance, a stacked classifier approach is employed.
4. *Key Detection*: Predictions on potential key-containing slices are made using the model, followed by a brute-force extraction.

SmartKex not only outperforms the brute-force method in speed but also excels in accuracy. Its applications span across cybersecurity and memory forensics. The adaptability of its machine learning methodology makes it a valuable asset for both researchers and professionals. The project's open-source nature further enhances its accessibility, with the code available on GitHub.

4.3 Our Contribution

In this research, we delve deep into the realm of SSH key detection by exploring multiple embedding techniques: graph-based, statistical-based, and deep learning-based embeddings. Our approach is twofold. Firstly, we employ these embeddings in conjunction with a classifier model, comparing their performance to determine the most effective method for SSH key extraction from memory heap dumps. Secondly, to address the challenges of consistency across various OpenSSH versions and usages, we implement a clustering approach. This ensures that our embeddings not only accurately detect SSH keys but also maintain coherence and adaptability across different OpenSSH environments.

5 Background

Building upon our exploration of SSH key detection, we recognize that OpenSSH plays a pivotal role in secure communication. The heap dumps of OpenSSH, essentially memory snapshots, are rich reservoirs of data. By generating graphs from these dumps, intricate connections between data structures, identified via their malloc headers, and their corresponding pointers are revealed.

Our research delves into the intelligent embedding of connections derived from OpenSSH heap dumps. Beyond mere graph representations, it's essential to comprehend the raw byte sequences within these dumps. Traditional methods such as Shannon entropy, Byte Frequency Distribution (BFD), and bigram frequencies form the foundation. However, the rise of deep learning has ushered in a range of sophisticated techniques. Models like Recurrent Neural Networks (RNN) [20] (including Long Short-Term Memory (LSTM)[14] and Gated Recurrent Units (GRU)[5]), sequence-to-sequence learning [31], and convolutional approaches (CNN)[21] offer novel perspectives on raw byte embedding. The integration of CNN with recurrent networks has proven effective in sequence modeling [2]. Furthermore, neural networks, especially in lossless representations, have shown promise in file fragment classification [12]. Our exploration also encompasses the potential of transformers[33] and autoencoders.

To identify structures containing OpenSSH keys, we employ machine learning classifiers. Among the standard models, the Random Forest classifier stands out for its versatility and accuracy. Balancing strategies are crucial, especially when dealing with imbalanced datasets, to ensure that the classifier doesn't exhibit bias towards the majority class. In addition to classification, our research emphasizes clusterization techniques to group similar data points and ensure coherence. Algorithms such as DBSCAN and OPTICS are at the forefront of our clusterization approach, providing insights into the inherent groupings within the OpenSSH heap dump data.

The aim of this background section is to provide a comprehensive overview of graph creation from heap dumps, techniques for raw byte embedding, and their role in identifying OpenSSH key structures. By merging age-old techniques with modern approaches, we strive to highlight the most effective methods for analyzing OpenSSH heap dump.

5.1 Traditional Statistical Embedding

Within the domain of machine learning, how data is represented significantly impacts the performance of models. Even though traditional statistical embedding techniques have been around before many contemporary methods, they continue to be vital in readying data for machine learning endeavors. Rooted in statistical foundations, these techniques provide a methodical approach to transform raw data into concise and meaningful forms. In this subsection, we'll delve into the nuances of entropy and its role in byte sequence embedding, Byte Frequency Distribution (BFD), and also highlight other classical statistical embedding methods pivotal in data representation for machine learning.

5.1.1 Entropy and its application in byte sequence embedding

Entropy, a fundamental concept in information theory, quantifies the amount of uncertainty or randomness associated with a set of data. Introduced by Claude Shannon in his groundbreaking work [30], entropy serves as a measure of the average information content one can expect to gain from observing a random variable's value.

Mathematically, the entropy $H(X)$ of a discrete random variable X with possible values $\{x_1, x_2, \ldots, x_n\}$ and probability mass function $P(X)$ is given by:

$$H(X) = -\sum_{i=1}^{n} P(x_i) \log_2 P(x_i) \tag{5.1}$$

Within the scope of identifying SSH keys, the significance of entropy cannot be understated. Byte sequences exhibiting high entropy typically reflect a multifaceted and varied informational content, traits that are synonymous with encryption keys, especially those in SSH. Sequences with pronounced entropy are often prime contenders for SSH keys due to their inherent randomness and lack of predictability, mirroring the attributes of robust security keys.

Fundamentally, entropy acts as a quantitative tool to evaluate the depth of information within data. When applied to SSH, it suggests that data sequences with elevated entropy levels have a heightened probability of correlating with secure keys. This positions entropy as an essential instrument for pinpointing and authenticating SSH keys.

5.1.2 Byte Frequency Distribution (BFD)

In the complex world of raw byte embedding, Byte Frequency Distribution (BFD) and n-gram embedding stand out as essential methods, each bringing unique benefits to data representation. BFD zeroes in on the distribution of individual byte values in a raw byte sequence. Analyzing these distributions allows for the identification of patterns that reflect the inherent nature of the data. This embedding technique becomes particularly relevant when assessing the randomness or structure of byte sequences, such as when detecting encrypted data or pinpointing specific file signatures.

On the other hand, n-gram embedding dives deeper into raw byte sequences. Instead of focusing solely on individual bytes, it captures patterns formed by sequences of 'n' consecutive bytes. This approach garners a wider range of contextual information from the raw byte data. For example, a trigram (3-gram) examines patterns formed by three sequential bytes, providing a richer representation than single byte values. Yet, a challenge with n-gram embedding is the potential for the output vector size to grow exponentially as 'n' increases, posing computational and storage issues, especially in real-time scenarios.

In the realm of raw byte embedding, both BFD and n-gram techniques offer invaluable perspectives. While BFD establishes a base representation centered on individual byte frequencies, n-gram embedding enhances it by spotlighting the complex relationships and patterns among consecutive bytes. Together, they form a robust arsenal for representing and analyzing raw byte data in a variety of applications.

5.1.3 Other traditional statistical embedding techniques

Mean Byte Value The Mean Byte Value represents the average value of all bytes in a given sequence. It provides an insight into the central tendency of the byte values in the sequence. Mathematically, for a byte sequence B of length n:

$$\text{Mean Byte Value} = \frac{1}{n}\sum_{i=1}^{n} B_i \tag{5.2}$$

Mean Absolute Deviation (MAD) MAD measures the average distance of each byte value from the mean, providing a sense of the dispersion or spread of the byte values around the mean. It is given by:

$$\text{MAD} = \frac{1}{n}\sum_{i=1}^{n} |B_i - \text{Mean Byte Value}| \tag{5.3}$$

Standard Deviation Standard Deviation quantifies the amount of variation or dispersion in the byte sequence. A higher value indicates greater variability in the byte values. It is defined as:

$$\text{Standard Deviation} = \sqrt{\frac{1}{n}\sum_{i=1}^{n}(B_i - \text{Mean Byte Value})^2} \tag{5.4}$$

Skewness Skewness[35] measures the asymmetry of the distribution of byte values around the mean. A positive value indicates a distribution that is skewed to the right, while a negative value indicates a distribution skewed to the left. It provides insights into the shape of the distribution of byte values. The Fisher's skewness[4] is :

$$\text{Skewness} = \frac{n}{(n-1)(n-2)}\sum_{i=1}^{n}\left(\frac{B_i - \text{Mean Byte Value}}{\text{Standard Deviation}}\right)^3 \tag{5.5}$$

Kurtosis Kurtosis[35] measures the "tailedness" of the distribution of byte values. A higher kurtosis value indicates a distribution with heavier tails, while a lower value indicates lighter tails. It provides insights into the extremities of the distribution. The Fisher's kurtosis[4] is :

$$\text{Kurtosis} = \frac{n(n+1)}{(n-1)(n-2)(n-3)}\sum_{i=1}^{n}\left(\frac{B_i - \text{Mean Byte Value}}{\text{Standard Deviation}}\right)^4 - \frac{3(n-1)^2}{(n-2)(n-3)} \tag{5.6}$$

n-gram on Bits When applying n-gram techniques to bits instead of bytes, we focus on sequences of 'n' consecutive bits. For example, a 2-gram on bits would consider patterns formed by two consecutive bits, resulting in four possible combinations: 00, 01, 10, and 11. This approach significantly reduces the size of the output vector compared to byte-based n-grams. By focusing on bits, we can capture more granular patterns in the data while benefiting from a more compact representation, which is computationally efficient and requires less storage.

5.2 Deep Learning Models for Raw Byte Embedding

In the area of data representation, deep learning is great for understanding raw byte sequences. Just like these models are good at understanding text, they're also good at understanding raw bytes. They can learn and show sequences on their own, which is really helpful for both text and raw bytes. In this section, we'll look at different deep learning models and how they work with raw byte embedding.

Our exploration begins with Word2Vec, a renowned technique for textual representation. Next, we'll delve into Recurrent Neural Networks (RNN). These networks, celebrated for their handling of word sequences in textual contexts, are equally adept with raw byte sequences. Moving forward, we'll discuss Convolutional Neural Networks (CNN), recognized for identifying patterns in raw bytes, a skill reminiscent of their proficiency with text. We'll subsequently introduce Autoencoders, distinguished by their distinctive learning paradigm. To round off this section, we'll examine Transformers, lauded for their expertise in capturing extended data relationships, much like their prowess with textual content.

5.2.1 Word2Vec: A Deep Dive into Word Embeddings

Word2Vec [24] is a groundbreaking algorithm in the realm of natural language processing (NLP) that transformed words into continuous vector spaces. Developed by Tomas Mikolov and his team at Google in 2013, this algorithm is based on the idea that the meaning of a word can be inferred by the context in which it appears.

5.2.1.1 Architectures

Word2Vec operates using one of two neural network architectures:

1. **Continuous Bag of Words (CBOW)**: This model predicts a target word based on its surrounding context. Given a context (a set of surrounding words), CBOW tries to predict the word that appears in the middle.

2. **Skip-Gram**: This is the inverse of CBOW. For a given word, the Skip-Gram model tries to predict the surrounding words (context). It can be visualized as predicting the 'context' from a 'word'.

5.2.1.2 Mechanism

Under the hood, Word2Vec uses a shallow neural network with a single hidden layer. However, the objective is not to achieve high accuracy in prediction but rather to learn rich word vector representations. Once trained, the weights of the hidden layer represent the word vectors.

Training proceeds as follows:

- Start with large amounts of text data and construct a vocabulary.
- For each word, create pairs of the word with its surrounding context words based on a defined window size.
- Use these pairs as input-output mappings to train the neural network.

5.2.1.3 Key Concepts and Innovations

1. **Distributional Hypothesis**: Word2Vec thrives on the idea that words appearing in similar contexts have related meanings. By analyzing vast amounts of text, the algorithm detects patterns and semantic relationships.
2. **Vector Arithmetic**: One of the most exciting outcomes of Word2Vec is its ability to perform vector arithmetic that captures semantic relationships. For example, the operation : $\text{vector}(\text{“}king''\text{)} - \text{vector}(\text{“}man''\text{)} + \text{vector}(\text{“}woman''\text{)}$ results in a vector close to $\text{vector}(\text{“}queen''\text{)}$.
3. **Subsampling and Negative Sampling**: To make training more efficient, Word2Vec introduced techniques like subsampling frequent words and negative sampling. Subsampling reduces the occurrences of high-frequency words in training, while negative sampling changes the training objective to distinguish the target word from randomly sampled 'negative' words.
4. **Word Analogies**: Word2Vec embeddings capture various dimensions of word meanings, leading to the discovery of word analogies. For example, $man : woman :: king : queen$ is a typical analogy captured by Word2Vec embeddings.

5.2.1.4 Applications

Word2Vec has paved the way for many NLP applications, including:

- **Semantic Word Similarity**: Comparing the cosine similarity of word vectors provides a measure of semantic similarity.
- **Information Retrieval**: Search engines can use word embeddings to better understand query intent and document content.

- **Sentiment Analysis**: Word embeddings capture sentiment dimensions, making them useful for sentiment classification tasks.
- **Machine Translation**: Word embeddings can act as a bridge between languages, aiding in tasks like machine translation.

5.2.1.5 Conclusion

Word2Vec was a significant leap forward in the domain of NLP, offering a mechanism to capture deep semantic word relationships in a computationally efficient manner. By viewing arbitrary long byte sequences as sentences, it becomes possible to adapt the Word2Vec algorithm for purposes beyond traditional text, broadening its applicability to our context.

5.2.2 RNNs : Understanding sequence data

Recurrent Neural Networks (RNN) are great tools for text classification. They're good at understanding the deeper meanings in text. Unlike older models that use hand-made features, RNN can learn and show sequences on their own. This makes them really useful for tasks that deal with sequences. When we think about embedding raw bytes, RNN's skill in understanding sequences is similar to how they handle word sequences in text. Here is a list of different RNN models and their advantages and disadvantages.

Recurrent Convolutional Neural Network (RCNN) for Text Classification[20]: The RCNN model, as discussed in the paper by Lai et al., is designed specifically for text classification. Unlike traditional models, RCNN do not rely on handcrafted features. Instead, they employ a recurrent structure to capture contextual information about words. This approach is believed to introduce considerably less noise compared to traditional window-based neural networks. The model's bidirectional structure ensures that both preceding and succeeding contexts of a word are considered, enhancing its understanding of the word's semantics.

- **Advantages:**
  - No need for handcrafted features.
  - Captures richer contextual information.
  - less noisy.
- **Disadvantages:**
  - Complexity due to bidirectional structure.
  - Might require more computational resources.

;

Long Short-Term Memory (LSTM)[14]: The LSTM, introduced by Hochreiter and Schmidhuber, is a specialized form of RNN designed to combat the vanishing gradient problem inherent in traditional RNN. The vanishing gradient problem arises when gradients of the loss function, which are used to update the network's weights, become too small for effective learning. This typically happens in deep networks or when processing long sequences, causing the earlier layers or time steps to receive minimal updates. As a result, traditional RNN struggle to learn long-term dependencies in the data.

LSTM address this issue with their unique cell state and gating mechanisms. The cell state acts as a "conveyor belt" that can carry information across long sequences with minimal changes, ensuring that long-term dependencies are captured. The gating mechanisms, namely the input, forget, and output gates, regulate the flow of information into, out of, and within the cell. This design allows LSTMs to selectively remember or forget information, making them adept at learning and retaining long-term dependencies in sequences.

- **Advantages:**
  - Efficiently learns long-term dependencies; overcomes the vanishing gradient problem inherent in traditional RNN.
  - Often achieves faster and more stable learning.
- **Disadvantages:**
  - More complex architecture compared to basic RNN and even GRU.
  - Can be computationally intensive due to the multiple gating mechanisms.

Gated Recurrent Units (GRU)[5]: GRU are a variant of RNN that aim to capture long-term dependencies without the complexity of LSTM. They use a gating mechanism to control the flow of information, making them efficient in sequence modeling tasks.

- **Advantages:**
  - Simplified structure compared to LSTM.
  - Efficient in capturing long-term dependencies.
  - Sometimes outperforms LSTM.
- **Disadvantages:**
  - Still more complex than traditional RNN.
  - Might not always outperform LSTM in all tasks.

To sum it up, RNN are good at understanding sequences and context. This makes them a good choice for embedding raw bytes. Just like they understand words based on the words around them, RNN can find patterns in raw byte sequences, giving us a better understanding of the data.

5.2.3 CNNs : Pattern detection in raw bytes

Convolutional Neural Networks (CNN)[21] are a specialized category of deep learning models adept at identifying patterns. Originally designed for visual data, their prowess extends to tasks like image and document recognition. Drawing inspiration from the human visual cortex's biological processes, CNN are architected to autonomously and adaptively discern spatial feature hierarchies from inputs. This becomes particularly relevant when considering raw byte embedding, where the goal is to detect patterns in sequences of bytes. The CNN architecture boasts convolutional layers that perform operations on input data to capture localized patterns, and pooling layers that condense spatial dimensions while preserving crucial information. This layered approach enables CNN to detect intricate patterns by progressively building on simpler foundational patterns. When applied to byte sequences or document recognition, CNN excel, showcasing remarkable efficacy, especially in tasks like identifying patterns within raw byte sequences or recognizing handwritten content.

When tailored to CNN, the Sequence-to-Sequence (Seq2Seq)[10] approach emerges as a potent tool for transforming raw byte sequences into meaningful embeddings. The encoder segment of the Seq2Seq model is central to this transformation. It delves into the byte sequence, discerning intricate patterns and nuances, and distills this rich information into a concise context vector or embedding. This condensed representation captures the core essence of the byte sequence, positioning it as a valuable input for subsequent tasks, such as classification models.

At the heart of the encoder lie the convolutional layers, skilled in pinpointing specific patterns within the byte sequence. Whether it's unique byte combinations or indicative n-grams, these layers are primed to detect them. As they traverse the raw byte sequence, they employ specialized filters, honed to recognize these specific patterns. As the data flows through the encoder's layers, these identified patterns are synthesized and refined, culminating in a comprehensive embedding of the sequence.

Here are two Sequence-to-Sequence (Seq2Seq) models using CNN :

- **Autoencoders:** These neural network architectures[13] are designed for data compression and reconstruction. The encoder part compresses the input data into a compact representation, while the decoder reconstructs the original data from this representation. In the context of raw byte sequences, the encoder can be used to generate embeddings that capture the essential patterns and structures of the data.

- **Transformers :** Transformers[33] utilize self-attention mechanisms to weigh the significance of different parts of the input data. This allows them to capture long-range dependencies and relationships in the data. When applied to raw byte sequences, transformers can generate embeddings that consider both local and global patterns, making them particularly effective for tasks that require understanding the broader context of a sequence.

Yet, a significant challenge with traditional Sequence-to-Sequence (Seq2Seq) models using CNN is their constraint in managing inputs of varying sizes. Constructed with a set input size, they face difficulties when presented with sequences of diverse lengths, like raw byte sequences.

To address this limitation, various techniques have been employed to normalize the size of the input data. One of the most common methods is **padding**, where shorter sequences are filled with predefined placeholder values (often zeros) until they match the length of the longest sequence in the dataset. This ensures that all sequences fed into the model have a uniform length. Another approach is **bucketing**, where sequences of similar lengths are grouped together, minimizing the amount of padding required. Additionally, **truncation** can be used to shorten sequences that exceed a certain length, although this might result in the loss of some information. While these techniques enable CNN-based Sequence-to-Sequence (Seq2Seq) models to handle variable-sized inputs, it's crucial to ensure that the preprocessing steps do not introduce noise or distort the inherent patterns and relationships within the raw byte sequences.

5.2.4 The Transformer Architecture

The Transformer [33] brought a novel approach to handling sequential data without relying on traditional recurrent mechanisms. Instead, it leverages attention mechanisms to draw global dependencies between input and output, achieving state-of-the-art results in a variety of NLP tasks.

5.2.4.1 Architecture Overview

The Transformer architecture is primarily composed of an encoder-decoder structure. Both the encoder and decoder consist of a series of identical layers, each with two primary components: multi-head self-attention and a position-wise feed-forward network.

5.2.4.2 Encoder

1. **Multi-Head Self-Attention**: This mechanism allows the model to focus on different parts of the input text simultaneously. It computes attention weights for different positions in the sequence, enabling the model to capture long-range dependencies.
2. **Position-wise Feed-Forward Networks**: After the attention scores are computed, they are passed through a feed-forward network, applied independently to each position.

5.2.4.3 Decoder

The decoder has an additional layer compared to the encoder:

1. **Multi-Head Self-Attention**: Functions similarly to the encoder.

2. **Multi-Head Cross-Attention**: This attends to the encoder's output.
3. **Position-wise Feed-Forward Networks**.

5.2.4.4 Attention Mechanism

At the core of the Transformer model lies the attention mechanism, a novel approach to capturing contextual information in sequences. This mechanism facilitates the model's ability to focus variably on different parts of the input, depending on the context. This context-sensitive focusing is achieved by computing a weighted sum of values, with the weights determined by the interaction between a query and a set of key-value pairs.

The Transformer employs a variant known as the "scaled dot-product attention". This attention mechanism can be understood through the following steps:

1. **Dot Product**: For each query, its dot product with all keys is computed. This results in a score that signifies the relevance of the query with respect to each key. Higher dot product values imply higher relevance.
2. **Scaling**: The scores obtained from the dot product are then scaled down by dividing them with the square root of the dimensionality of the query and key vectors. This scaling is crucial because for larger magnitudes of the dot products, the softmax 5.3.1 function would squash its inputs causing a very small gradient – essentially a very hard softmax. Scaling counteracts this potential issue, ensuring a softer softmax where the gradient is larger.
3. **Softmax Normalization**: The scaled scores for each query are then passed through a softmax operation. This operation ensures that the scores are normalized and lie between 0 and 1, making them interpretable as probabilities. These probabilities dictate how much attention should be given to each corresponding value in the sequence.
4. **Weighted Sum of Values**: Lastly, the softmax normalized scores are used to take a weighted sum of the values. The result of this weighted sum gives the output of the attention mechanism for the given query. If a specific key is highly relevant to the query (i.e., has a high softmax score), then the corresponding value will have a larger weight in the final sum.

The beauty of this mechanism is that it allows the Transformer to consider multiple parts of the input sequence when producing an output, rather than being limited to a fixed window or relying on recurrent state. By attending variably to different input parts based on context, the Transformer can capture complex patterns and long-range dependencies in the data.

5.2.4.5 Multi-Head Attention

Instead of performing a single set of attention computations, the Transformer utilizes multiple sets (or "heads"). Each head learns different attention weights, and their outputs are concatenated and

linearly transformed to produce the final result.

5.2.4.6 Positional Encoding

In traditional recurrent architectures such as RNNs and LSTMs, the inherent recurrence mechanism enables the model to naturally take into account the order or sequence of tokens. The Transformer architecture, in stark contrast, relies entirely on self-attention mechanisms which, in their basic form, are order-agnostic. This means that without any additional information, shuffling the input tokens would produce the same output. To address this limitation and introduce the notion of order or sequence into the architecture, positional encodings are ingeniously integrated into the Transformer's design.

The positional encodings are added to the initial embeddings of tokens before they are processed by the encoder and decoder stacks. These encodings are designed such that they can provide a unique representation for each token based on its position in the sequence, regardless of the token's actual value. This ensures that the model can distinguish between tokens not just based on their content, but also based on their positions.

The positional encodings utilize sinusoidal functions, specifically sine and cosine functions, of varying frequencies. For a position p and a dimension i, the encoding is defined as:

$$PE_{(p,2i)} = \sin\left(\frac{p}{10000^{\frac{2i}{d}}}\right)$$

and

$$PE_{(p,2i+1)} = \cos\left(\frac{p}{10000^{\frac{2i}{d}}}\right)$$

where d is the dimension of the embeddings. This formulation ensures that each position produces a distinct and consistent encoding. Moreover, because of the geometric progression in the denominators, these functions create encodings that can be easily differentiated by the model across positions, providing a relative sense of position between tokens.

Using sinusoidal functions as positional encodings comes with the advantage that these encodings can be scaled to accommodate sequences of varying lengths, even beyond those seen during training. This is because the sum of the positional encoding and token embedding will result in a unique and consistent value, allowing the model to generalize to different sequence lengths. Intuitively, the sinusoidal nature of the encodings creates a pattern that the model can learn, helping it understand relative positions and distances between tokens in a sequence.

5.2.5 Benefits and Applications

- **Parallelization**: Without recurrent layers, the Transformer can process all tokens in the input sequence simultaneously, making it amenable to parallel processing and reducing training times.

- **Long-range Dependencies**: The self-attention mechanism can, in theory, relate distant words in a sequence, capturing long-term dependencies without relying on the sequence's length.

- **Flexibility**: The architecture is not inherently sequential, making it adaptable to a variety of tasks beyond NLP.

5.2.6 Conclusion

The Transformer architecture, with its focus on attention mechanisms, has set new standards in the realm of deep learning for sequential data. It serves as the foundation for various state-of-the-art models in NLP, such as BERT, GPT, and T5, underscoring its significance and versatility in the field.

5.3 Machine learning

Machine learning, an integral part of artificial intelligence, revolves around designing algorithms and statistical models that allow computers to perform tasks without being directly programmed. Instead of relying on detailed instructions for every task, machine learning techniques empower systems to learn from data and make data-driven decisions. A key method in this field is supervised learning, in which models are trained using data that comes with predefined labels. Here, each piece of data in the training set has an associated known output. The primary goal of supervised learning is to establish a relationship between inputs and outputs, enabling the model to predict or categorize new, unseen data based on this relationship.

A cornerstone in this realm is feature engineering, which involves the meticulous process of selecting and transforming variables to optimize model performance. Another challenge frequently encountered by practitioners is dealing with datasets where some classes are overrepresented, which can skew model predictions. Among the myriad of machine learning models available, certain ones have gained prominence due to their versatility and effectiveness. We will provide an overview of some of these notable models.

5.3.1 Softmax Function

The softmax function is an essential component in machine learning, especially for classification tasks. It is responsible for converting a vector of real numbers into a probability distribution.

5.3.1.1 Definition

Given a vector $\mathbf{z} = [z_1, z_2, ..., z_K]$ of real numbers, the softmax function S is defined for each element z_i as:

$$S(z_i) = \frac{e^{z_i}}{\sum_{j=1}^{K} e^{z_j}} \tag{5.7}$$

where:

- e is the base of natural logarithm.
- K represents the number of classes or the dimensionality of the vector.

5.3.1.2 Intuition

1. **Exponentiation**: Each element of the vector is raised to the power of e. This ensures that all resulting elements are non-negative and exaggerates the differences between them. A significantly larger value will have an exponentially greater value compared to a smaller one after this operation.
2. **Normalization**: The exponential values are divided by their sum. This step ensures that the output values lie in the range [0, 1], and their total sums up to 1, hence forming a valid probability distribution.

5.3.1.3 Applications in Machine Learning

In classification problems, the raw outputs from a model (typically from the last layer of a neural network) are real numbers that do not necessarily sum up to one. The softmax function converts these raw scores into a probability distribution over the categories. In most cases, the category with the highest probability post the softmax operation is taken as the model's prediction.

For instance, in a neural network tasked with recognizing handwritten digits ranging from 0 to 9, the final layer might produce a 10-dimensional vector. Applying softmax on this vector gives a probability distribution over these ten digits. The digit corresponding to the highest probability after softmax is then chosen as the model's prediction.

5.3.2 Features engineering

Feature engineering[16] is a cornerstone in the realm of machine learning. It involves the artful transformation of the given feature space to optimize the performance of predictive models. The significance of feature engineering cannot be overstated; it serves as a bridge between raw data and the predictive models, ensuring that the models are fed with the most relevant and informative features. Properly engineered features can drastically reduce modeling errors, leading to more accurate and reliable predictions. Here are some of the most common feature engineering techniques:

- **Normalization and Scaling** are preprocessing techniques used to standardize the range of independent features in the data. Many machine learning algorithms, especially those that rely on distance calculations like k-means clustering or support vector machines, are sensitive to the scale of the data. If features are on different scales, one feature might dominate others, leading to suboptimal model performance. Normalization typically scales features so that they have a unit norm, while other scaling methods, such as Min-Max scaling, transform features to lie in a given range, usually [0,1]. Z-score normalization or standard scaling is another method where features are scaled based on their mean and standard deviation. Properly scaled data ensures that each feature contributes equally to the model's decision, leading to more stable and accurate predictions.

- **Interaction Features[15]** refer to the creation of new features by combining two or more existing features, aiming to capture any synergistic effect between them. In many cases, the interaction between variables can provide more information than the individual variables themselves. For instance, while analyzing real estate prices, the individual features 'number of rooms' and 'location' might be informative, but their interaction, 'number of rooms in a specific location', might offer even more predictive power. Interaction features can be created by multiplying, adding, or even dividing original features, and they can help in capturing non-linear relationships in the data, enhancing the model's ability to make accurate predictions.

- **Feature Selection[15]** is a critical process in the machine learning pipeline that focuses on selecting the most relevant features from the original set, aiming to reduce the dimensionality and improve model performance. The primary goal is to eliminate redundant or irrelevant features that don't contribute significantly to the predictive power of the model. This not only helps in reducing the computational cost but also can lead to a more interpretable model. There are various techniques for feature selection, including filter methods (based on statistical measures), wrapper methods (like recursive feature elimination), and embedded methods (where algorithms inherently perform feature selection, such as decision trees). By judiciously selecting features, one can build efficient models that are less prone to overfitting and have better generalization capabilities.

5.3.2.1 Correlation tests

To assess feature quality, various statistical measures come into play, including correlation tests that gauge the strength and direction of relationships between variables. Pearson, Kendall, and Spearman correlation coefficients are frequently employed to quantify linear or monotonic associations between each feature and the target variable [3]. A high absolute value of these coefficients indicates a robust relationship, aiding in feature selection.

- **Pearson Correlation:** This measures linear relationships between two variables, ranging from -1 to 1. -1 signifies a strong negative linear correlation, 1 suggests a strong positive linear correlation, and 0 implies no linear correlation.

- **Kendall's Tau:** This non-parametric test gauges the strength and direction of a monotonic relationship between two variables.

- **Spearman's Rank:** Also non-parametric, it assesses how well an arbitrary monotonic function can describe the relationship between two variables without making assumptions about frequency distribution.

These techniques are valuable for evaluating relationships between each feature and generating correlation matrices, which, in turn, help identify redundant features. Univariate feature selection techniques allow the evaluation of each feature independently. In Python's scikit-learn library [26], methods like the F-test value and p-value are often used for this purpose.

- **F-test value:** This measures the linear dependency between the feature variable and the target. A higher F-test value suggests a more useful feature.
- **p-value:** It indicates the probability of an F-test value as large as observed arising if the null hypothesis is true. A smaller p-value implies rejecting the null hypothesis, indicating the feature's significance.

In summary, features constitute the foundational elements of any machine learning model. The quality of these features, their processing, and utilization significantly impact the model's performance. Feature engineering is of paramount importance, as properly engineered features can substantially reduce modeling errors, leading to more accurate and reliable predictions. It serves as a crucial link between raw data and predictive models, ensuring that models are fed with the most relevant and informative features.

5.3.2.2 Dimensionnality reduction

Following the aforementioned techniques, another essential facet in the feature engineering landscape is dimensionality reduction. As data grows in complexity, it often encompasses a vast number of features, leading to what is known as a high-dimensional space. While a plethora of features might seem advantageous, it introduces challenges, notably the *curse of dimensionality*[34, 17]. In such high-dimensional realms, data points tend to become increasingly sparse. This sparsity means that the relative distances between data points start to appear uniform, making it arduous for algorithms to discern meaningful patterns. This can lead to models that overfit the training data, capturing noise rather than the underlying data distribution. Additionally, the computational overhead increases, and deriving intuitive insights from the data becomes a daunting task.

Dimensionality reduction techniques come to the rescue by striving to trim down the number of features while preserving the crux of the information. Techniques like Principal Component Analysis (PCA) and t-Distributed Stochastic Neighbor Embedding (t-SNE) are employed to transform the data from its original high-dimensional space to a more manageable, lower-dimensional one. This transformation aims to retain the significant patterns and structures inherent in the data. By judiciously reducing the dimensionality, not only can models be trained more efficiently, but they often yield bet-

ter performance by focusing on the most pertinent features. This streamlined approach mitigates the challenges posed by the curse of dimensionality, ensuring models that are both robust and interpretable.

5.3.3 Imbalanced data

In machine learning, a frequent obstacle is the presence of datasets where one category vastly overshadows others[28]. This imbalance can skew models towards predicting the dominant class, often neglecting the less prevalent but potentially more critical class.

To counteract this, a variety of techniques have been devised:

- **Resampling:** This encompasses both increasing instances of the minority class (oversampling) and decreasing instances of the majority class (undersampling). A notable method for oversampling is the Synthetic Minority Over-sampling Technique (SMOTE), which generates artificial data points in the feature space.
- **Weighted Loss:** This strategy involves assigning greater weights to the minority class during the training phase, ensuring the model gives it due consideration.
- **Ensemble Methods:** Approaches such as bagging and boosting can be tailored to ensure a balanced class representation. For example, in bagging, each sample can be structured to maintain a balanced class ratio.
- **Anomaly Detection:** This method reframes the task from classification to anomaly detection, viewing the minority class as an outlier or anomaly.

Selecting an appropriate strategy hinges on the specific problem and dataset characteristics. It's also crucial to evaluate the model's efficacy using suitable metrics, ensuring it genuinely addresses the imbalance.

5.3.4 Some common models

- **Logistic Regression[25] :** Logistic regression serves as a statistical technique tailored for binary classification tasks. While linear regression is designed to forecast continuous outcomes, logistic regression focuses on predicting the likelihood of a binary result. It leverages the logistic function to relate multiple independent variables to a binary outcome, ensuring the predicted values fall between 0 and 1. Typically, a 0.5 threshold is used to classify the final outcome. A key strength of logistic regression is its clarity and ease of interpretation, though it might face challenges with complex non-linear data unless further feature adjustments are made.
- **Decision Trees[18] :** Decision trees are machine learning models designed for both classification and regression tasks. They segment data into subsets based on feature values, making decisions at each node. While their hierarchical structure offers easy visualization and interpretation, they

can be prone to overfitting. However, strategies like pruning can help in refining the tree and mitigating overfitting.

- **Random Forest[27] :** Random Forest is an ensemble method that creates a 'forest' of decision trees. Each tree is trained on a random subset of the data and makes its own predictions. The Random Forest algorithm then aggregates these predictions to produce a final result. This method is known for its high accuracy, ability to handle large datasets with higher dimensionality, and its capacity to manage missing values.
- **Support Vector Machines (SVM)[36] :** SVM are used for both regression and classification problems. They work by finding the hyperplane that best divides a dataset into classes. SVMs are effective in high-dimensional spaces and are versatile, as different Kernel functions can be specified for the decision function.
- **K-Nearest Neighbors (KNN)[19] :**KNN is a simple, instance-based learning algorithm. To make a prediction for a new data point, the algorithm finds the 'k' training examples that are closest to the point and returns the most common output value among them.

5.3.5 Random Forest classifier model

Random Forest, as introduced earlier, is an ensemble learning method that operates by constructing multiple decision trees during training and outputting the mode of the classes for classification tasks or mean prediction for regression tasks. Let's delve deeper into its workings, advantages, and disadvantages.

5.3.5.1 How Random Forest Works

1. **Bootstrap Aggregating (Bagging):** Random Forest begins by creating multiple datasets using bagging. It randomly selects samples from the original dataset with replacement, ensuring diversity in the datasets.
2. **Constructing Decision Trees:** For each of these datasets, a decision tree is constructed. However, instead of using all features to make a decision at a node, a random subset of features is chosen. This introduces further randomness into the model and ensures that the trees are uncorrelated.
3. **Aggregation:** Once all the trees are constructed, predictions are made by each tree. For classification, the mode of all the predictions is taken as the final prediction.

5.3.5.2 Advantages of Random Forest

- **Accuracy:** Random Forests often produce highly accurate predictions as they combine the output of multiple decision trees.
- **Overfitting:** The model is less prone to overfitting due to the randomness introduced in its construction.

- **Handling Missing Data:** Random Forest can handle missing values by either using median values to replace continuous variables or computing the proximity-weighted average of missing values.
- **Feature Importance:** It provides insights into the importance of different features in making predictions.

5.3.5.3 Disadvantages of Random Forest

- **Complexity:** Random Forest creates a lot of trees (unlike only one tree in the case of decision tree) and combines their outputs. This makes the model more complex and computationally intensive.
- **Longer Training Time:** Due to the construction of multiple trees, the training time can be longer compared to other algorithms.
- **Less Intuitive:** While individual decision trees are simple and can be visualized, a forest is more challenging to interpret due to its ensemble nature.

In conclusion, while Random Forest offers high accuracy and is robust against overfitting, it comes with increased complexity and training time. However, its advantages often outweigh the disadvantages, making it a popular choice for various machine learning tasks.

5.4 Clustering

Clustering is a key technique in unsupervised machine learning, aiming to group similar data points together. It's all about ensuring that items within a cluster are more alike than those in different clusters. This approach is great for uncovering hidden patterns in data. When it comes to checking the quality of an embedding, clustering can be a handy tool. By forming clusters from embedded data, we can see how effectively similar structures come together. A top-notch embedding should make sure that data points from the same structure cluster closely. So, by looking at how well clustering works, we can gauge the strength of the embedding.

5.4.1 K-Means Clustering

K-Means [23] is a popular clustering method recognized for its straightforwardness and speed. It works by dividing a dataset into 'K' unique, separate groups (or clusters) based on how close each data point is to the cluster's center, termed the centroid. The method repeatedly places each data point with the closest centroid and then updates the centroid's position based on the points in its cluster. This cycle repeats until the centroids no longer move significantly. Though K-Means is great for clusters that are roughly spherical and similar in size, deciding on the best number of clusters (K) in advance can be tricky.

5.4.2 DBSCAN

DBSCAN [8] is a clustering method that identifies dense regions in data, considering sparse areas as outliers. Unlike K-Means, DBSCAN doesn't need a pre-defined number of clusters. It works on the principle that a cluster is a high-density area in data, surrounded by less dense regions. The algorithm is steered by two key parameters: the minimum points needed for a region to be dense and a distance measure determining how close points should be to create a cluster. DBSCAN shines in handling datasets where clusters have varying shapes but similar densities.

5.4.3 Spectral Clustering

Spectral clustering[22] is a method that emphasizes reducing the dimensionality of data using the eigenvalues of a similarity matrix. By constructing a similarity graph, where nodes represent data points and edges carry weights based on point similarities, the technique transforms the original space. Utilizing the eigenvectors of the graph's Laplacian, it creates a more compact and manageable representation. In this reduced space, traditional clustering methods like K-Means become more effective. Spectral clustering's strength lies in its ability to handle complex cluster structures, especially non-convex clusters, making it a valuable tool for diverse applications.

5.4.4 OPTICS Clustering

Ordering Points To Identify the Clustering Structure (OPTICS) [1] is an advanced density-based clustering algorithm that was introduced as an extension to DBSCAN. The primary motivation behind OPTICS was to address some of the limitations of DBSCAN, especially its sensitivity to the global density parameter. Let's dive deeper into the workings, advantages, and disadvantages of OPTICS.

5.4.4.1 How OPTICS Works

1. **Ordering of Data Points:** OPTICS begins by processing each data point in the dataset. For each point, it computes its reachability distance with respect to other points. This distance is based on the density of the data, and it gives an indication of how close or far a point is from a dense region.

2. **Reachability Plot:** The reachability distances for all points are then used to create a reachability plot. This plot provides a visualization of the density-based clustering structure of the data. Peaks in the plot represent sparse regions, while valleys correspond to dense clusters.

3. **Cluster Extraction:** Clusters can be extracted from the reachability plot by analyzing its valleys. Points within a valley belong to the same cluster. The depth and shape of a valley give insights into the density and shape of the cluster.

5.4.4.2 Advantages of OPTICS

- **Varying Densities:** Unlike DBSCAN, which struggles with clusters of varying densities, OPTICS can identify clusters that have different density levels within the same dataset.
- **No Global Density Parameter:** OPTICS does not require a global density threshold, making it more adaptive to the data's inherent structure.
- **Visualization:** The reachability plot provides a visual representation of the clustering structure, aiding in the interpretation of results.

5.4.4.3 Disadvantages of OPTICS

- **Complexity:** OPTICS is computationally more intensive than DBSCAN due to the ordering of data points and the generation of the reachability plot.
- **Interpretation:** While the reachability plot provides a visual representation, extracting clusters from it can be challenging and may require additional heuristics or methods.

5.4.4.4 Parameters of OPTICS

The OPTICS algorithm also provides a range of parameter choices to cater to different clustering needs:

- **clusterization method:**
  - `"xi"`: The ξ method, often referred to as the "steepness" method, is designed to extract clusters from the reachability plot generated by the OPTICS algorithm. The reachability plot is a visualization where data points are plotted based on their reachability distances. In this plot, clusters manifest as valleys, and the depth or steepness of these valleys indicates the density of the cluster. The ξ method works by:
    * Identifying regions in the reachability plot where there is a significant change in the reachability distance, indicating potential cluster boundaries.
    * Determining the "steepness" of these regions. A region is considered steep if the relative change in reachability distance exceeds a threshold, typically denoted by the parameter ξ.
    * Extracting clusters based on these steep regions. Clusters are formed by connecting steep upward regions (representing the start of a cluster) with steep downward regions (indicating the end of a cluster).
    * Handling noise: Points that do not belong to any of the identified steep regions are typically considered as noise or outliers.

    The advantage of the ξ method is its ability to detect clusters of varying densities without the need for specifying the number of clusters in advance. However, the choice of the ξ

parameter can influence the granularity of the clustering, with smaller values leading to more fine-grained clusters and larger values resulting in coarser clusters.

- Other methods: Include the DBSCAN-equivalent method and others, each offering a unique approach to cluster extraction.

- **clusterization metrics:**

  - `"cosine"`: Cosine similarity is a metric used to determine the cosine of the angle between two non-zero vectors in an inner product space. It is especially suitable for high-dimensional datasets, such as text data represented as vector space models or TF-IDF vectors. The cosine similarity, $\text{sim}(A, B)$, between two vectors A and B is given by:

$$\text{sim}(A, B) = \cos(\theta) = \frac{A \cdot B}{\|A\|\|B\|} \tag{5.8}$$

    where:

    * θ is the angle between vectors A and B.
    * $A \cdot B$ represents the dot product of the vectors.
    * $\|A\|$ and $\|B\|$ denote the magnitudes (or norms) of vectors A and B, respectively.
    * **Advantages**:
      · *Scalability*: Cosine similarity is less affected by the magnitude of vectors, making it advantageous for data that doesn't scale linearly. This means that even if the data is not normalized, cosine similarity can still provide meaningful results.
      · *High-dimensional data*: In high-dimensional spaces, Euclidean distances can become inflated, a phenomenon known as the "curse of dimensionality." Cosine similarity, on the other hand, remains robust in such scenarios, making it a preferred choice for datasets with many features.
      · *Sparse data*: For datasets where vectors are sparse (i.e., have many zeros), cosine similarity can be more efficient and meaningful than other distance metrics. This is because it focuses on the orientation (angle) between vectors rather than their absolute differences.

  - Other metrics: Include Euclidean, Manhattan, Jaccard, and more, each with its distinct advantages.

- **clusterization algorithm:**

  - `"brute"`: Employs the brute-force approach to compute pairwise distances, ensuring exact distance calculations (allow cosine metrics).
  - Other algorithms: Such as "kd-tree" or "ball-tree", which can offer faster computations for specific datasets.

In conclusion, OPTICS offers a more flexible approach to density-based clustering compared to DBSCAN. Its ability to handle clusters of varying densities and its adaptive nature make it a powerful tool for clustering tasks. However, its increased computational complexity and challenges in cluster extraction require careful consideration.

5.5 Dataset

SmartKex has enriched the research domain by curating an extensive annotated dataset of OpenSSH heap memory dumps, which is publicly accessible on Zenodo[1] [9].

The dataset is systematically structured into three primary directories: *Training*, *Validation*, and *Performance_Test*. Both the *Training* and *Validation* directories are further segmented based on distinct SSH scenarios, including immediate exit, port-forward, secure copy, and shared connection. Each scenario directory is then subdivided according to the OpenSSH version that produced the memory dump. Within these version-specific directories, heap dumps are organized by their respective key lengths, offering a hierarchical structure that facilitates targeted research explorations.

Figure 5.1: Schematic Representation of the Dataset's Directory Hierarchy

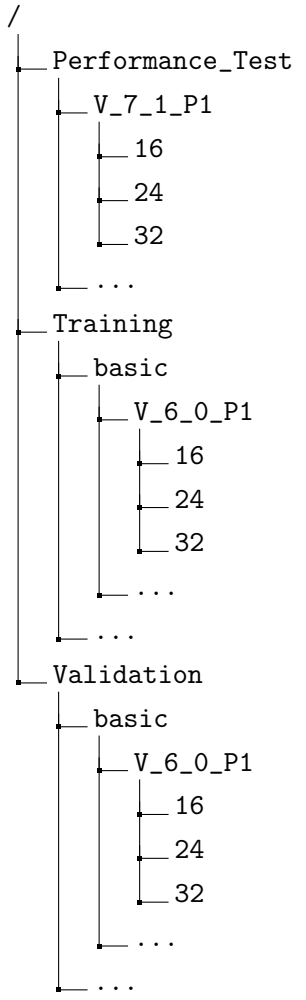

The dataset predominantly employs two file formats: JSON and RAW. While the JSON files encapsulate meta-data such as the encryption technique, the virtual memory address of the key, and its hexadecimal representation, the RAW files house the actual memory dump of the OpenSSH process.

[1] `https://zenodo.org/record/6537904`

5.5.1 Details of the Dataset Production System

While the [9] paper and the associated dataset do not explicitly detail the hardware and software configurations used during its creation, such information is pivotal. This is especially true as our analysis delves into allocated raw bytes, which are influenced by the underlying system and the C library in use. To bridge this information gap, we reached out to the authors directly.

In correspondence with Dr. Hans Reiser, we were provided with specifics about the system used to generate the dataset. The system's configuration was ascertained using the following command outputs:

```
root@debian10:~# ldd --version
ldd (Debian GLIBC 2.28-10) 2.28
Copyright (C) 2018 Free Software Foundation, Inc.
This is free software; see the source for copying conditions.
     There is NO
warranty; not even for MERCHANTABILITY or FITNESS FOR A
   PARTICULAR PURPOSE.
Written by Roland McGrath and Ulrich Drepper.
```

Code 5.1: C-library version utilized during dataset generation

```
root@debian10:~# lsb_release -a
No LSB modules are available.
Distributor ID:     Debian
Description:        Debian GNU/Linux 10 (buster)
Release:            10
Codename:           buster
```

Code 5.2: Linux Standard Base Release details

```
root@debian10:~# uname -a
Linux debian10 4.19.0-16-amd64 #1 SMP Debian 4.19.181-1
   (2021-03-19) x86_64 GNU/Linux
```

Code 5.3: Operating system and kernel version details

Dr. Reiser further mentioned that the dataset was produced on a system powered by an Intel Xeon CPU, specifically either the E5-2609 or the E3-1230 model. Based on the provided commands, we can summarize the system's key attributes as:

- **CPU architecture:** `x86_64`
- **Operating System:** `Debian GNU/Linux 10 (buster)`
- **Kernel version:** `4.19.0-16-amd64`
- **C library version:** `Debian GLIBC 2.28-10`

5.5.2 C structures and chunks allocation understanding

Given that the dataset encompasses entire heap dump files, it presents an opportunity to identify potential data structures within these dumps. Identifying these structures involves searching for patterns within the heap dump. However, when it comes to data structures, our insights into the C library in use become invaluable, guiding our search.

OpenSSH, being crafted in C, naturally embeds C data structures within its heap dumps. In C, memory allocation for data structures is typically handled by the `malloc` function. This function, when invoked, allocates memory corresponding to the size of the specified data structure and returns a pointer to this allocated space (also call chunks). Given our knowledge that the dataset was generated with `GLIBC 2.28` 5.5.1, a dive into the `malloc` function within `GLIBC 2.28` reveals a noteworthy detail. The comments within the code mention that each allocated chunk carries a minimal overhead, either 4 or 8 bytes, which holds size and status details [11]. This overhead is what we term the *malloc header*. Consequently, we can anticipate the presence of 8-byte aligned blocks within the heap dump that aren't pointers but are remnants of a `malloc` invocation. Recognizing these *malloc headers* paves the way for detecting potential data structures within the heap dumps.

On a Linux system with a `x86_64` architecture, the `malloc` function typically employs a block (or chunk) header to store metadata about each allocated segment. Positioned right before the memory block returned to the user, the specifics of this header can vary based on the C library's implementation (e.g., glibc, musl). However, it generally encapsulates:

- **Size of the Block**: This represents the allocated block's size, typically denoted in bytes. Often, this size encompasses the header's size and might be aligned to multiples of 8 or 16 bytes.
- **Flags**: These are a set of indicators that shed light on the block's status. They can signify if the block is free or allocated, or even if the preceding block is free or allocated. Ingeniously, these flags are often stashed in the size field's least significant bits, leveraging the alignment of the size which zeroes out these bits.

5.5.3 Understanding `malloc` in Heap Memory Allocation

The `malloc` function, as implemented in GLIBC 2.28, employs a boundary tag methodology to oversee memory chunks. Each of these chunks incorporates metadata essential for both memory allocation and deallocation [11] [6].

A chunk represents a continuous memory segment, typically comprising multiple 8-byte blocks, managed by `malloc`. The structure of a chunk encompasses the following elements [6] [32]:

1. **Size of Previous chunk**: Present only if the preceding chunk is free (with its `P` (PREV_INUSE) bit unset), this field assists in locating the start of the prior chunk.

2. **Size of chunk**: This captures the chunk's byte size and integrates three flags: `A` (NON_MAIN_ARENA), `M` (IS_MMAPPED), and `P` (PREV_INUSE). These flags reside in the size field's last three LSBs. This block is often referred to as the *malloc header* block in subsequent discussions.

3. **User Data**: The actual memory segment returned for user utilization.

4. **Size of Next chunk**: Represents the size of the succeeding contiguous chunk.

5. **Foot**: Mirrors the chunk's size and is reserved for application data.

6. **Flags**:

    - `A` (NON_MAIN_ARENA): Denotes if the chunk resides in the primary or a thread-specific arena.
    - `M` (IS_MMAPPED): Flags if the chunk was allocated via `mmap`.
    - `P` (PREV_INUSE): Signifies if the preceding chunk is occupied. If unset, the prior chunk is free.

The chunk allocation mechanism is underpinned by:

1. **Initialization**: The inaugural chunk allocated invariably has its `P` bit activated to avert accessing non-existent memory.

2. **Free chunks**: These chunks are cataloged in circular doubly-linked lists, encompassing forward and backward pointers for navigation.

3. **Mmapped chunks**: Such chunks, identifiable by the `M` bit in their size fields, are allocated individually.

4. **Fastbins**: Regarded as allocated chunks, their consolidation is executed collectively.

5. **Top chunk**: A unique chunk that perpetually exists. If it dwindles below `MINSIZE` bytes, it undergoes replenishment.

The code comments offer a detailed chunk representation, comprising 8-byte blocks [11]. It's worth noting that this representation is tailored to align with our forensic analysis needs. A subtle distinction lies in the `footer`'s portrayal, which, for our purposes, is deemed part of the succeeding chunk rather than the current one. The footer of the prior chunk essentially corresponds to the `mchunkptr` address. As elucidated in the GlicC wiki, a "chunk pointer" or `mchunkptr` doesn't point to the chunk's commencement but to the terminal word in the preceding chunk. This implies that the initial field in `mchunkptr` is valid only when the prior chunk is free [6]. Given the interplay between free and allocated chunks, it's more intuitive to perceive the footer as an element of the next chunk. This schematic representation divergence doesn't alter the actual data structure but merely offers a clearer visualization.

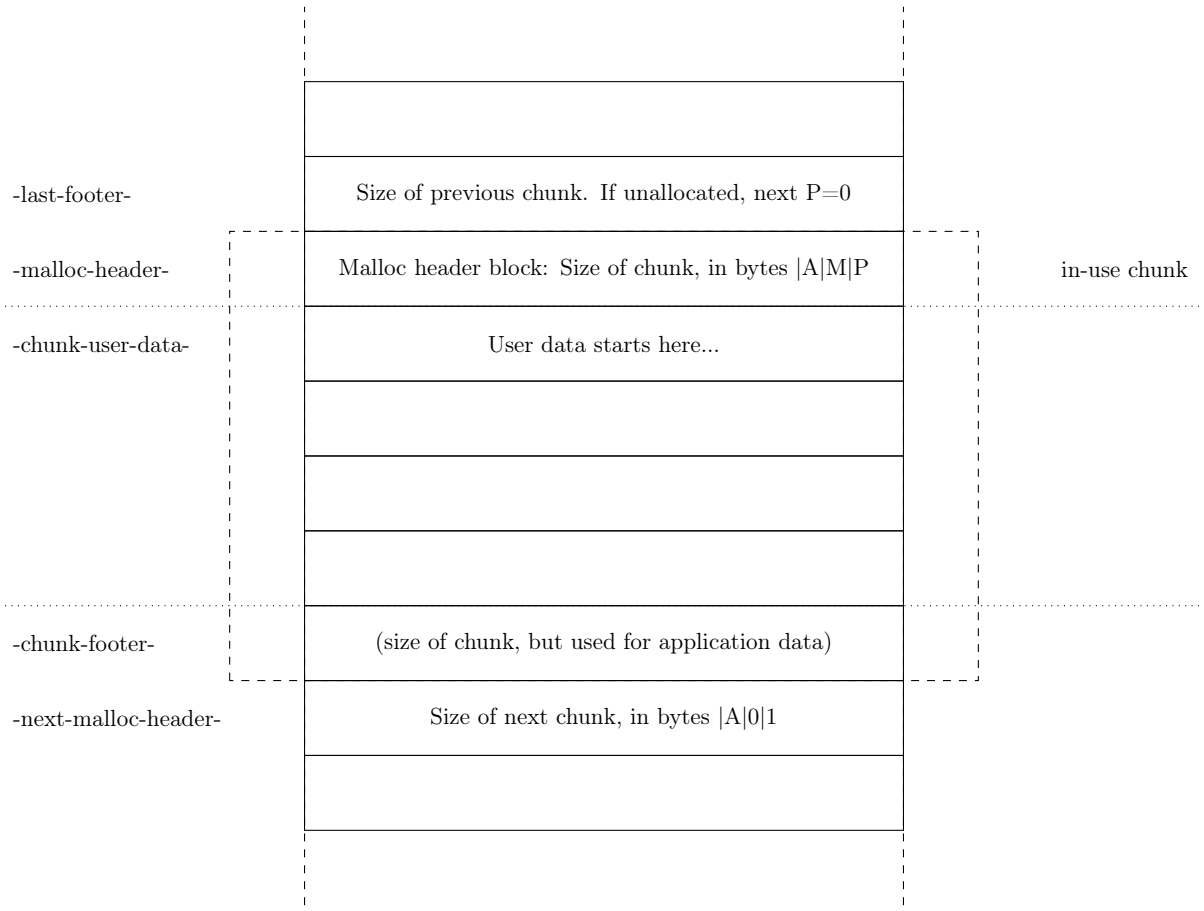

Figure 5.2: Diagram of an allocated chunk in GLIBC 2.28 [11].

In GLIBC 2.28, the `malloc` function employs a boundary tag approach to oversee memory chunks. These chunks integrate metadata essential for memory allocation and deallocation [11] [6]. The library organizes available chunks into circular doubly-linked lists, termed "bins", facilitating rapid retrieval of free memory chunks of specific sizes. However, these bins are not directly accessible in the heap dump file. To discern if a particular chunk is occupied or available, several techniques can be employed. Primarily, the `P` bit in the malloc header serves as an indicator. A value of 1 denotes an occupied chunk, while 0 signifies a free chunk.

It's noteworthy that certain heap dump files appear truncated, with the concluding block being incomplete and filled with zeros. An instance of this can be observed in the final chunk of *Training/basic/V_7_1_P1/24/17016-1643962152-heap.raw*.

```
1 WARN: chunk [94022266975200] Chunk(block_index=10876, size
     =48176, flags=[A=False, M=False, P=True]) is out of bounds.
     Last block index: 16895 Iteration index: 16896
2 WARN: chunk [94022266975200] Chunk(block_index=10876, size
     =48176, flags=[A=False, M=False, P=True]) is out of bounds.
     Last block index: 16895 Iteration index: 16897
3 Chunk(block_index=10876, size=48176) is only composed of zeros.
```

Code 5.4: Logs from chunk exploration script, highlighting the last chunk of the file *Training/basic/V_7_1_P1/24/17016-1643962152-heap.raw*.

A free chunk, as per the code documentation [11], incorporates pointers to the subsequent and preceding free chunks within the heap for its designated bin. The following provides a representation of a free chunk:

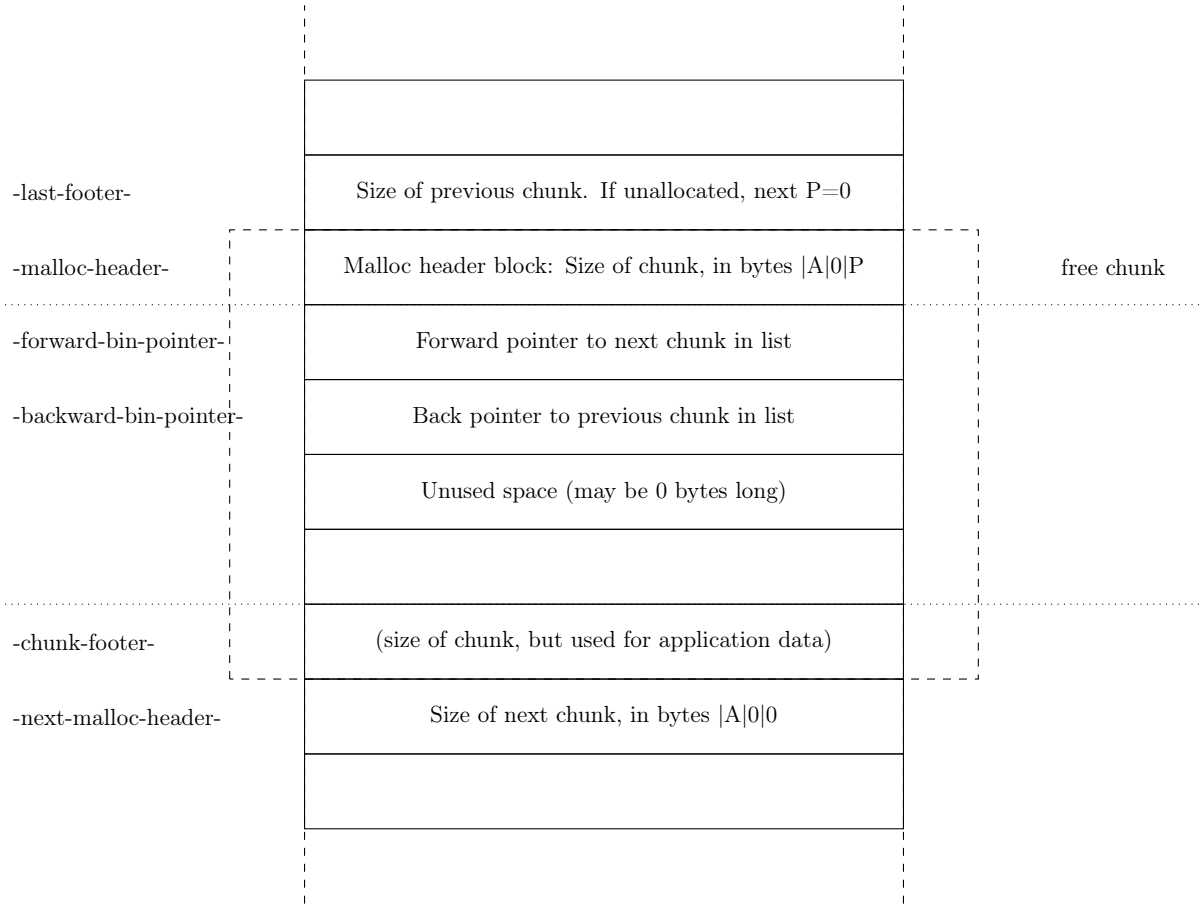

Figure 5.3: Diagram of a free chunk in GLIBC 2.28 [11].

The principle of **chunk chaining** is pivotal for navigating the heap dump file. By adhering to the sequence of malloc headers, we can systematically traverse the allocated memory chunks within the heap dump. This methodology is corroborated by the source code, which contains a comment indicating that, given the address of the initial chunk (the one with the lowest address) in a heap, one can iterate over all the chunks by leveraging the size data.

Throughout the development of scripts and tools for this thesis, we've integrated various checks and validations to ensure the consistency of this chunk chaining assumption. Should any discrepancies arise, the tools are designed to flag an error, and typically bypass the problematic data. Such a design choice aims to fortify the tools against unforeseen data structures and to bolster the reliability of the outcomes.

6 Methods

This research dives into the complexities of embedding byte sequences, focusing particularly on the extraction of structures containing SSH keys for machine learning purposes. The varied uses of OpenSSH introduce distinct challenges due to potential variations in the created embeddings. Given the wide array of SSH key dimensions and OpenSSH's intricate operations, maintaining the embeddings' stability and consistency is vital. In this methodological section, we will detail various embedding methods, present a framework for their assessment through a classifier model, and suggest another strategy to verify the embeddings' coherence between the different OpenSSH usage and key sizes.

6.1 Dataset

The dataset at the core of this thesis, as previously introduced (see 5.5), consists of heap dump raw files related to different OpenSSH use cases and versions. Each heap dump file is paired with a JSON annotation file created by the dataset's creators. These JSON files provide extra information about the heap dump, especially regarding encryption keys. In this section, we will explain our exploration of the dataset, aiming to better comprehend its content and nuances.

6.1.1 Origin

The dataset is derived from heap dumps that capture various OpenSSH usage scenarios. These scenarios encompass four distinct SSH interactions: a straightforward client connection to the server followed by an immediate exit, port-forwarding, secure copying, and SSH shared connection. The heap dumps span different OpenSSH versions and a range of key sizes, from 16 to 64 bytes. These dumps were generated using the SmartKex tool [9]. The data collection was conducted on a mini PC equipped with an AMD Ryzen 5500U processor, 16GB of RAM, and a 1TB NVMe SSD, running Debian 11 as its operating system.

6.1.2 Estimating the dataset balancing for key prediction

In this part, our primary objective was to assess the balance of the dataset for key prediction and identify the challenges associated with it.

To begin, we aimed to gain an understanding of the dataset's scale. We utilized a code snippet 6.1 to count all the files within the dataset, revealing a total of 208,745 files. However, it was imperative to recognize that JSON files, which served as annotation files, were not to be considered part of the raw bytes for embedding. Consequently, these JSON files were excluded from our count to provide a more accurate representation of the dataset's size.

```
1         find . -type f | wc -l
```

Code 6.1: Count all dataset files

Following this, we employed another code snippet 6.2 to specifically count the heap dump raw files, excluding JSON files. This count indicated a total of 103,595 heap dump raw files, which constituted the primary focus of our analysis.

```
1         find . -type f -name "*.raw" | wc -l
```

Code 6.2: Count heap dump raw dataset files

To gain further insights into the dataset, we determined its size while excluding annotation files 6.3. The calculated dataset size amounted to 18,067,001,344 bytes.

```
find . -type f -name "*.raw" -exec du -b {} + | awk '{s+=$1} END {
    print s}'
```

Code 6.3: Get the size of the dataset

Considering the nature of the dataset, which featured a maximum of six keys per file, each with a maximum size of 64 bytes, we conducted a rough estimate. We determined that the maximum number of bytes relevant for searching across the dataset was $6 * 64 * 103595 = 39780480$. This calculation accounted for approximately 0.22% of the dataset's total size.

Lastly, it is crucial to acknowledge that the dataset exhibited a significant imbalance and is very large. To address this challenge effectively, strategies were implemented to ensure robust, unbiased analyses, and scalability.

Annotations

The annotations files are essential to understand the data and how best to utilize them for the study. Each heap dump corresponds to one specific JSON file. To view the contents of these JSON files in a more organized manner, one can reference the method provided at 6.4. For a clearer understanding, an extract of the JSON annotation from the file located at `./Training/client/V_7_8_P1/16/13116-1644920217.json` is available at 6.5.

```
python3 -m json.tool file.json
```

Code 6.4: pretty print JSON

```
{
    /* file ./Training/client/V_7_8_P1/16/13116-1644920217.json
       */
    "SSH_STRUCT_ADDR": "5619dd7e5570",
    "SESSION_STATE_ADDR": "5619dd7e5df0",
    "KEY_A_ADDR": "5619dd807f40",
    "KEY_A_LEN": "12",
    "KEY_A_REAL_LEN": "12",
    "KEY_A": "34fbe182e76c49a617a93e2e",
    /*...*/
    "KEY_E_ADDR": "5619dd808000",
    "KEY_E_LEN": "0",
    "KEY_E_REAL_LEN": "0",
    "KEY_E": "",
    "KEY_F_ADDR": "5619dd807fd0",
    "KEY_F_LEN": "0",
    "KEY_F_REAL_LEN": "0",
/    "KEY_F": "",
    "HEAP_START": "5619dd7e3000"
}
```

Code 6.5: An extract of the JSON annotations

Within these annotation files, several critical pieces of information are present. The "SSH_STRUCT_ADDR" and "SESSION_STATE_ADDR" denote the addresses of vital openSSH structures. These addresses are pivotal in gauging the embedding coherence across different openSSH uses and key sizes. If the embeddings of these structures display similarity across various key sizes and openSSH usages, it signifies the embedding's coherence.

Other significant annotations such as "KEY_A_ADDR", "KEY_A_LEN", "KEY_A_REAL_LEN", and "KEY_A" detail the address, length, and value of the key A. In general, six of these annotations can be found for each heap dump. Notably, the "HEAP_START" annotation, along with the length of the heap dump, is of paramount importance. This annotation signifies the starting address of the heap dump. This information not only aids in pinpointing addresses in the heap dump for structures and pointers, but also refines the heuristic used in detecting pointers. By leveraging the "HEAP_START" information, one can verify if a pointer is pointing within the heap dump boundaries. As a practical illustration, deducing the address of key A within the heap dump can be achieved by subtracting "HEAP_START" from "KEY_A_ADDR".

However, it's noteworthy that some of these annotation files may be corrupted. Therefore, it's imperative to verify the integrity of each file before its use. In instances where keys are corrupted, such as "KEY_E" and "KEY_F" having no recorded values in the extract found at 6.5, it's advised either to remove the corrupted keys or discard the entire file if the data cannot be salvaged.

6.1.3 Dataset Validation

The dataset primarily consists of heap dump RAW files, each corresponding to various use cases and versions of OpenSSH. Accompanying each heap dump is a JSON annotation file, crafted by the dataset's creators, to furnish supplementary details, particularly about encryption keys.

However, the dataset isn't without its flaws. Its application in machine learning has unveiled certain inconsistencies. For example, a few of these files are incomplete, lacking essential data. This poses a challenge since we rely on these annotations to pinpoint key addresses, crucial for annotating memory graphs in the embedding phase. If there's a discrepancy in the format, we'll deem the JSON annotation as corrupted and bypass it. This likely stems from the automated generation of annotations. A case in point is the file in *Training/basic/V_7_8_P1/16/*, which, being the dataset's first file, showcases an incomplete annotation with absent keys. It's vital to be cognizant of these limitations when utilizing the dataset for academic endeavors.

6.1.3.1 Annotation Integrity Verification

To accurately gauge the usability of the dataset for machine learning applications, we implemented a validation script named `check_annotations.py`. This script is tailored to assess the annotations for their quality, completeness, and consistency.

The annotations (JSON files) are categorized as follows:

- **Complete and Accurate Files**: These files are devoid of missing keys and contain all keys with appropriate values.
- **Malformed Files**: These are files that aren't valid JSON and hence cannot be loaded properly.
- **Inconsistent Files**: Files that present conflicting information within their annotations.
- **Files with Absent Keys**: These files lack certain keys in their annotations. For instance, a JSON file might have "KEY_E": "", indicating the absence of key E and its corresponding address in the annotation, which poses challenges for accurate machine learning labeling.
- **Files with Incomplete Keys**: These files contain keys but lack the corresponding addresses. An example would be a JSON file with "KEY_E": "689e549a80ce4be95d8b742e36a229bf", signifying the presence of key E but the absence of its address in the annotation. This again complicates the labeling process for machine learning.

The script executes swiftly, processing all the 103,595 JSON annotation files and yields the following outcomes:

- **Correct and Complete Files**: 26,196 files.

- **Broken Files**: 6 files are identified as broken. Closer inspection reveals these files to be empty.
- **Incorrect Files**: 0 files.
- **Files with Absent Keys**: 58,643 files exhibit missing keys.
- **Files with Incomplete Keys**: 18,750 files display incomplete keys.

Delving deeper into the keys:

- **Total SSH Keys**: 546,534 keys.
- **Missing (Empty) SSH Keys**: 157,244 keys.
- **Incompletely Annotated SSH Keys**: 37,500 keys.
- **Incorrectly Annotated SSH Keys**: 0 keys.

6.1.4 Structure of the Heap File

Heap files serve as the dynamic memory storage for applications, and understanding their structure is crucial for memory analysis. These files are organized in a specific manner, with memory sequences of bytes or "chunks" allocated and deallocated as needed by the application. The heap is 8-byte aligned, which means that we can consider sequences of memory in 8-byte block. This alignment ensures efficient memory access and management. To visualize and interpret the heap's structure, tools like memory analyzers or debuggers can be employed.

Within the heap, there are four primary types of byte sequences that can be identified with varying degrees of certainty:

1. **Chunk, Malloc Header, and Footer**: We have already discussed these components in detail in an earlier section. In brief, they represent the primary building blocks of the heap, with each chunk being a segment of memory allocated for storing data. The malloc header contains essential metadata about the chunk, and footers, when present, replicate this information.
2. **Pointer**: Memory addresses that reference other locations within the heap or other memory segments.

Any unidentified user data within these structures is termed as "value data." This data represents the actual content or payload stored within the allocated memory chunks.

6.1.4.1 Chunk

In our exploration of the dataset, the chunk chaining assumption, as detailed in section 5.5.3, plays a pivotal role. It's imperative to ensure the integrity of this assumption for accurate analysis. During the dataset refinement process, we identified five heap dumps that contain chunks with a size of 0 bytes, which could potentially violate this assumption. To maintain the reliability of our analyses, these specific dumps have been removed from the dataset.

6.1.4.2 Pointer

Pointers are memory addresses that reference other locations within the heap or other segments of memory. In the context of the heap, pointers can indicate data structures, reference other chunks, or provide links in data structures like linked lists or trees. To identify potential pointers within the heap dump, one can utilize the following Reggex :

```
1 :/[0-9a-f]\{12}0\{4}
```

This command searches for sequences comprising 12 hexadecimal characters succeeded by 4 zeros. The rationale behind this is twofold:

- The heap dump file's maximum possible addresses typically span around 12 hexadecimal digits.
- Pointers' addresses are represented in little-endian format. Consequently, the address's last 4 bytes at 0 are its Most Significant Bytes (MSB).

Furthermore, with knowledge of the heap's start addresses and the dump's size, we can enhance the precision of our search. By doing so, we can exclude potential pointers that point outside the boundaries of the dump. Another refinement can be made by verifying if the values pointed to by the potential pointers are 8 bytes aligned, as the heap is structured in 8-byte sequences. However, it's crucial to note that this approach remains heuristic in nature. As such, there's still a possibility of detecting blocks that aren't genuine pointers.

6.1.4.3 Footer

In the GLIBC documentation, the footer of a chunk is expected to mirror the chunk's size as indicated in the malloc header. However, an inconsistency is observed: the size stated in the footer block doesn't always align with this expectation. This deviation is consistently seen across the refined dataset.

6.1.5 Heap File Distribution

The dataset offers an in-depth perspective on heap dumps, systematically sorted by key size, OpenSSH version, and distinct use cases. This methodical arrangement streamlines the analytical

process, enabling precise investigations tailored to particular criteria. In the subsequent sections, we'll delve into the distribution of the dataset, emphasizing the file count across different use cases, versions, and key sizes, to ensure its suitability for consistent testing.

6.1.5.1 Full Dataset

In our initial phase of exploration, we will concentrate on the full dataset. This comprehensive analysis will provide a holistic understanding of the data's structure, variations, and potential anomalies.

- A unique instance was observed where a folder was devoid of any content. This was in the Training section, specifically for the client use case, version V_7_8_P1, and a key size of 64 bytes.
- In the Training segment, which comprises 82 combinations of use cases, versions, and key sizes:
  - The minimum number of RAW files present is 923.
  - The maximum stretches to 1095. The difference between these two extremes is calculated as:
    $$\frac{\max - \min}{\min} = 0.186 \tag{6.1}$$
    This results in a 18.6% difference.
- For the Testing segment, which has 15 combinations:
  - The RAW files range from a minimum of 100 to a maximum of 101, marking a mere 1% difference between the two.
- The Validation segment, with its 82 combinations, shows:
  - A minimum of 151 RAW files.
  - A maximum of 211 RAW files. The difference between these values is:
    $$\frac{\max - \min}{\min} = 0.397 \tag{6.2}$$
    This presents a 39.7% difference, yet the number of files remains substantial enough to validate any model effectively.

The dataset, with its meticulous organization and vast range, offers a robust platform for in-depth analysis and model validation.

6.1.5.2 Clean Dataset

Following our examination of the full dataset, we will shift our focus to the cleaned dataset. This refined subset, having undergone meticulous preprocessing and filtering, will offer insights into the most pertinent and reliable data points. Analyzing the cleaned dataset will ensure that our conclusions and subsequent actions are based on high-quality, accurate data.

- In the Training segment, which comprises 82 combinations of use cases, versions, and key sizes:
  - 63 subdirectories are empty, with no RAW files present.
  - The minimum number of RAW files present is 923.
  - The maximum stretches to 1079. The difference between these two extremes is calculated as:
    $$\frac{\max - \min}{\min} = 0.169 \tag{6.3}$$
    This results in a 16.9% difference.
- For the Testing segment, which had 15 combinations : 0 subdirectories are empty, then no changes are observed.
- The Validation segment, with its 82 combinations, shows:
  - 62 subdirectories are empty, with no RAW files present.
  - A minimum of 151 RAW files.
  - A maximum of 209 RAW files. The difference between these values is:
    $$\frac{\max - \min}{\min} = 0.384 \tag{6.4}$$
    This presents a 38.4% difference, yet the number of files remains substantial enough to validate any model effectively.

The specifics of the empty folders, including their exact locations and other details, will be cataloged comprehensively in the annex C.1. It's crucial to note that due to the invalid nature of the data in these folders, our coherence study on the embeddings will not factor in the OpenSSH version, use case, or key size involved. This decision ensures that our analysis remains rooted in valid and meaningful data, thereby enhancing the reliability of our findings.

While the cleaning process did invalidate certain cases within the dataset, it's essential to emphasize that a significant portion remains intact and consequential. These preserved cases provide a robust foundation for our analysis, ensuring that our study is both comprehensive and grounded in meaningful data. The invalidated cases, though notable, do not diminish the overall value and depth of the dataset at our disposal.

6.1.6 Keys Analysis

The analysis of SSH keys within the heap dumps provides crucial insights into their characteristics and behaviors. These findings not only enhance our understanding of the data but also guide subsequent steps in the research process.

6.1.6.1 Keys Positions

Upon analyzing all the heap dumps, it became evident that all the SSH keys mentioned in the annotations are positioned at the beginning of their respective chunks. This consistent positioning greatly simplifies certain embedding processes and offers a streamlined approach to further analysis.

6.1.6.2 Keys Entropy

Another significant observation regarding the keys is their high entropy, as referenced in 4.2. High entropy is indicative of randomness, which is a characteristic feature of cryptographic keys. Leveraging this high entropy 5.1 can be instrumental in discriminating the keys from other data. However, it's essential to approach this method with caution. While high entropy can be a strong indicator, it's not foolproof. There's a possibility of encountering false positives, as other high entropy data might exist in the heap. Additionally, there might be instances of false negatives, especially when keys contain multiple repeated bytes by chance.

6.2 Embedding

Our next objective centers on the conversion of raw byte data into fixed-size embeddings (5.1, 5.2), a pivotal step in preparing them for utilization in machine learning applications. Ensuring uniformity in embedding size across all memory structures holds paramount significance. Consistency in embedding dimensions is vital to empower machine learning algorithms for efficient data processing and analysis. This uniformity not only simplifies the integration of memory structures with varying sizes into a coherent classification framework but also acts as a defense against the adverse effects of the curse of dimensionality—a phenomenon that can introduce computational complexities and heighten the risk of overfitting in high-dimensional data spaces. Striking this equilibrium is essential, achieved by maintaining reasonably low embedding dimensions, fostering both efficient data processing and the preservation of essential information within the raw byte data. It's important to note that initially, each embedding will include the structure's file and the structure's address in the file. However, these details will be removed during the machine learning phase (quality or coherence) as the embedding aims to be free of key size or OpenSSH uses. Their presence will serve as a means to test coherence later in our analysis.

6.2.1 Statistical embedding

Understanding the fundamental concepts of statistical embeddings enables us to delve deeper into the sophisticated processes and practical applications that underscore their significance in embedding tasks. By utilizing statistical techniques, data from high-dimensional spaces is condensed, preserving the inherent probabilistic connections and essential patterns as much as possible.

6.2.1.1 N-gram values

In reference to section 5.1.2, we adopt the use of n-gram values, specifically focusing on the frequency of byte combinations. However, an implication of this approach is that it leads to an exponentially high dimensional space. For instance, with a 2-gram, the potential values amount to $256 * 256 = 65536$. Given the extensive dimensionality, we have opted for combinations of bits rather than bytes. This change substantially reduces the space required; a 2-gram, in this case, would only amount to $2 * 2 = 4$ values.

Switching to bit combinations aligns well with our objectives. Our main interest is in the frequency patterns of n-gram values rather than the specific n-gram values themselves. This is because our core aim is to identify SSH keys, which inherently display frequencies for all combinations due to their random nature.

In our approach, we utilize 1-gram, 2-gram, and 3-gram values. As a result, our dimensional space is confined to 14 dimensions, as calculated by $2*2*2+2*2+2 = 14$. We believe this is an optimal trade-off, striking a balance between the size of the space and the richness of the information it encapsulates.

6.2.1.2 Other statisticals values

In our approach, several metrics are employed to analyze the data. Specifically, we utilize the mean as detailed in 5.2, the standard deviation as found in 5.4, the MAD from 5.3, the skewness as outlined in 5.5, the kurtosis referenced in 5.6, and the Shannon entropy from 5.1. These metrics, when collectively considered, provide a comprehensive understanding and embed a plethora of information about the data at hand.

It's imperative to note a particular aspect of our analysis concerning the standard deviation. There are instances where the standard deviation registers a value of zero. Such an occurrence is indicative of data consistency. Concurrently, in such scenarios, both the kurtosis and skewness are undefined. When faced with this situation, our course of action is to dismiss the chunk from our analysis. The rationale behind this is straightforward: a consistent chunk would likely not be pertinent to our exploration, especially when our aim is to identify patterns characteristic of an SSH key, wich are random by nature.

6.2.1.3 Statistical embedding

We employ then a combination of n-gram values and other statistical metrics to construct the vectors for each chunk. The n-gram approach contributes 14 distinct values to the vector. Simultaneously, the supplementary statistical metrics, which encapsulate measures of the mean, standard deviation, MAD, skewness, kurtosis, and Shannon entropy, introduce an additional 6 values. Consequently, the resultant vector for each structure comprises a total of 20 values.

6.2.2 Graph embedding

In this section, we shift our focus towards the creation and embedding of graphs derived from the heap dump data. The process of graph creation involves structuring the data in a way that captures the relationships and connections between the chunks and their pointers. Subsequently, we will transform this graphs into low-dimensional vector representations, enabling the application of machine learning techniques to identifying chunks containing ssh keys.

6.2.2.1 Graphs creation

Our graph construction is a meticulously organized process aimed at representing the intricate relationships present within the heap dump data. Comprising three distinct node types - chunks, pointers, and value nodes - this graph provides a comprehensive view of the data's structure. Our approach commences with the sequential parsing of the heap dump data, enabling the identification of essential chunks central to our analytical objectives. These chunks form the core nodes of our graph. To establish connections between these chunks and the data they contain, we further divide each structure into 8-byte blocks, which is the size of the heap alignment. These blocks are then translated into value nodes within the graph, serving as connectors bridging the data structures to their specific data. An heuristic approach, grounded in REGEX 6.1.4.2, is employed to identify valid pointers within

the heap dump data, with pointers representing a subset of value nodes, indicating legitimate pointers references. The scrupulously established connections between chunks, value nodes, and pointers ensure that the graph accurately mirrors the intricate relationships found within the heap dump data. This comprehensive graph construction process is efficiently implemented in Rust, making effective use of the Petgraph library to handle the complexities of heap dump data and graph representation, offering superior efficiency compared to a Python-based implementation.

In the following image 6.1, we can see the chunks nodes representing in blue, containing pointers nodes in orange and value nodes nodes in gray.

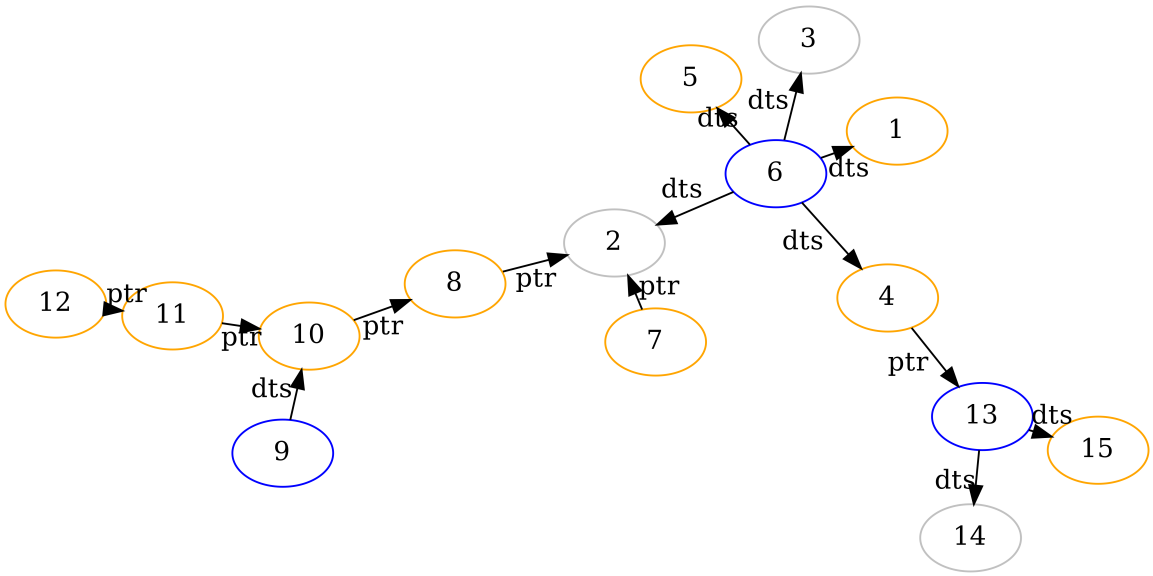

Figure 6.1: Graph creation process

After the construction of the graph, we can use graphviz (and the DOT language)[7] to visualize the graph, using the command :

```
sfdp -Gsize=67! -Goverlap=prism -Tpng dot_file > image.png
```

The following image is an example of the creation of the graph from the file `./Validation/Validation/basic/V_8_1_P1/24/27107-1643980590-heap.raw` without value nodes to enhance clarity.

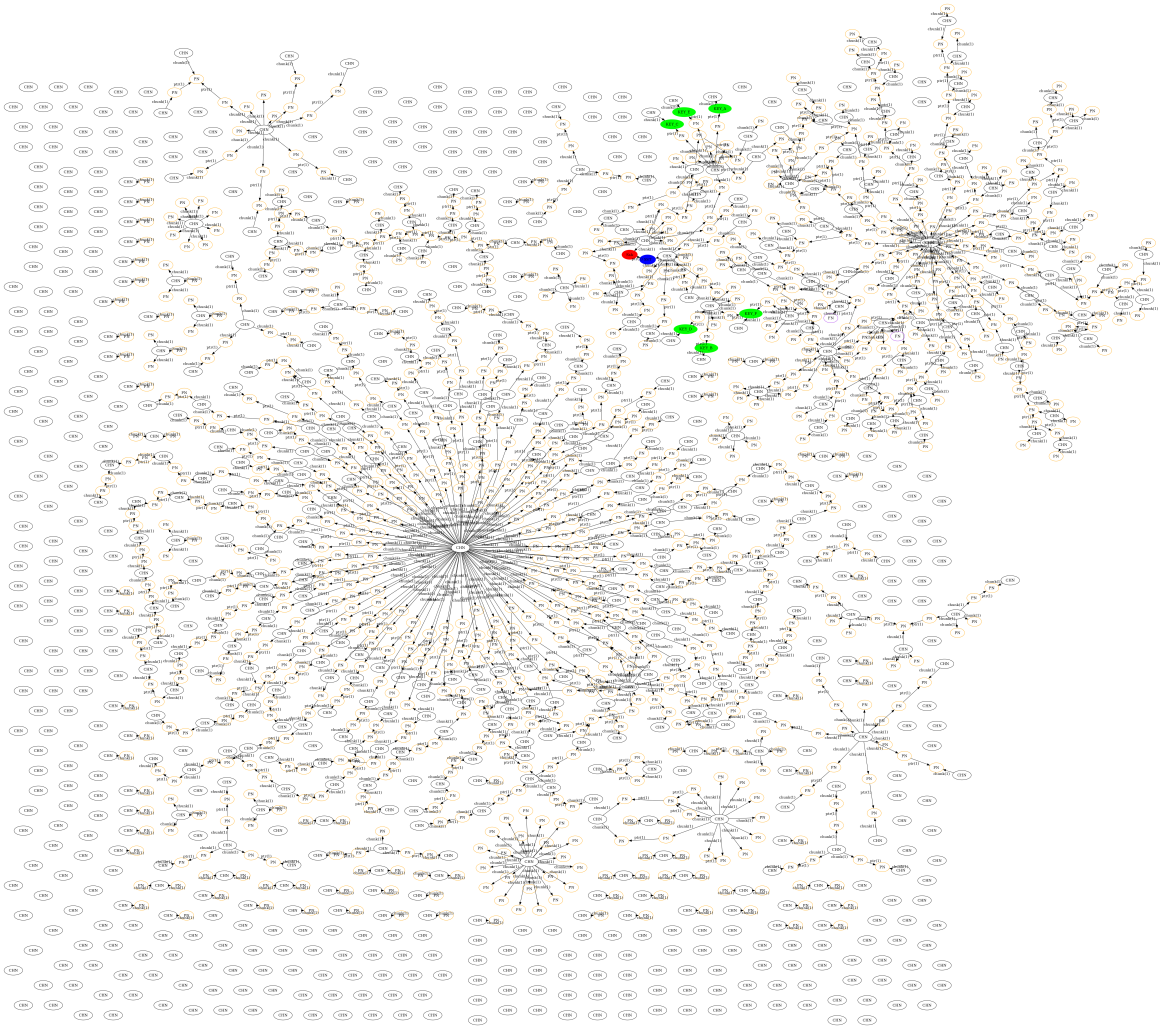

Figure 6.2: Graph example

6.2.2.2 Graphs embedding

Our next step is to uncover deeper insights and semantic understanding from our constructed graph, focusing on semantic embedding. This is the process through which we reshape our graph into a low-dimensional vector space, with each vector acting as a repository for a chunk's immediate neighborhood. Through this transformative journey, our aim is to forge vector representations that empower the application of cutting-edge machine learning techniques.

To create a concise yet informative representation, considering both structure-to-member and pointer-based connections, we meticulously count the number of pointers and chunks directly referencing a specific chunk's members. This initial count provides valuable insights into the chunk's immediate context. However, we doesn't stop there; we expand this representation by including counts of pointers and chunks pointing to those preceding nodes, allowing us to capture deeper layers of context. This recursive process continues until we reach a predetermined depth. Furthermore, we initiate a parallel analysis in reverse, meticulously tracing connections by following pointers from the initial chunk to capture its children, recursively delving deeper until we reach the specified depth. We can see the algorithm here 6.6. The result is a low-dimensional vector that intricately encodes the chunk's

neighborhood, offering a comprehensive view of its relationships and contextual significance within the graph.

Algorithm 6.6 Generate Ancestor/Children Embedding

```
function GenerateNeighborsDTN(structure_node, dir)
    ancestor_nodes ← an empty set
    children ← graph.neighbors_directed(structure_node, OUT)   ▷ Get members of the structure
    for child in children do
        ancestor_nodes.insert(child)
    end for
    result ← an empty list
    current_nodes ← an empty set
    for _ in 0 to DEPTH do
        current_nodes ← ancestor_nodes                ▷ switch ancestor nodes and current nodes
        ancestor_nodes ← an empty set
        nb_dtn ← 0
        nb_ptr ← 0
        for current_node in current_nodes do
            if node is DataStructureNode then          ▷ Update number of structures and pointers
                nb_dtn ← nb_dtn + 1
            else if node is PointerNode then
                nb_ptr ← nb_ptr + 1
            end if                                          ▷ Get neighbors of the current node
            for neighbor in graph.neighbors_directed(current_node, dir) do
                ancestor_nodes.insert(neighbor)        ▷ Add neighbors to the next ancestor nodes
            end for
        end for
        result.append(nb_dtn)                                ▷ Add number of data structures
        result.append(nb_ptr)                                    ▷ Add number of pointers
    end for
    return result
end function
```

We can apply this algorithm to every chunk within each graph, delving to a depth of 8, which produces an embedding of 32 units: 8 for ancestor pointers, 8 for ancestor chunks, 8 for child pointers, and 8 for child chunks. To accurately represent the chunk's neighborhood, it's crucial not to omit details about its members. Thus, we incorporate the count of pointers in the members and the chunk's dimensions. This results in a final embedding size of 34 - 32 for the neighborhood and an additional 2 for the chunk size and pointer count. However, there are inherent challenges with this embedding. It tends to get polluted by the value node, which often lacks significant meaning. Moreover, the relationships between the structures are intricate, and there's potential to represent them in a more straightforward manner, as show in the next section.

6.2.2.3 Updated graph

Recognizing these challenges and the need for a clearer representation, we embarked on a series of refinements. Our approach focuses on enhancing the last graph by preserving the structure nodes and their interconnections via pointers. To simplify the visualization, we've decided to eliminate both the

value nodes and the pointer nodes. In addition, the relationships that previously connected the pointer nodes to the value nodes will now link directly to the chunk nodes, with the added detail of weighted edges. This strategy is driven by our aspiration to offer a more lucid graph, significantly reducing any extraneous noise, as show in the figure 6.3, the representation of the file *14911-1644326802*.

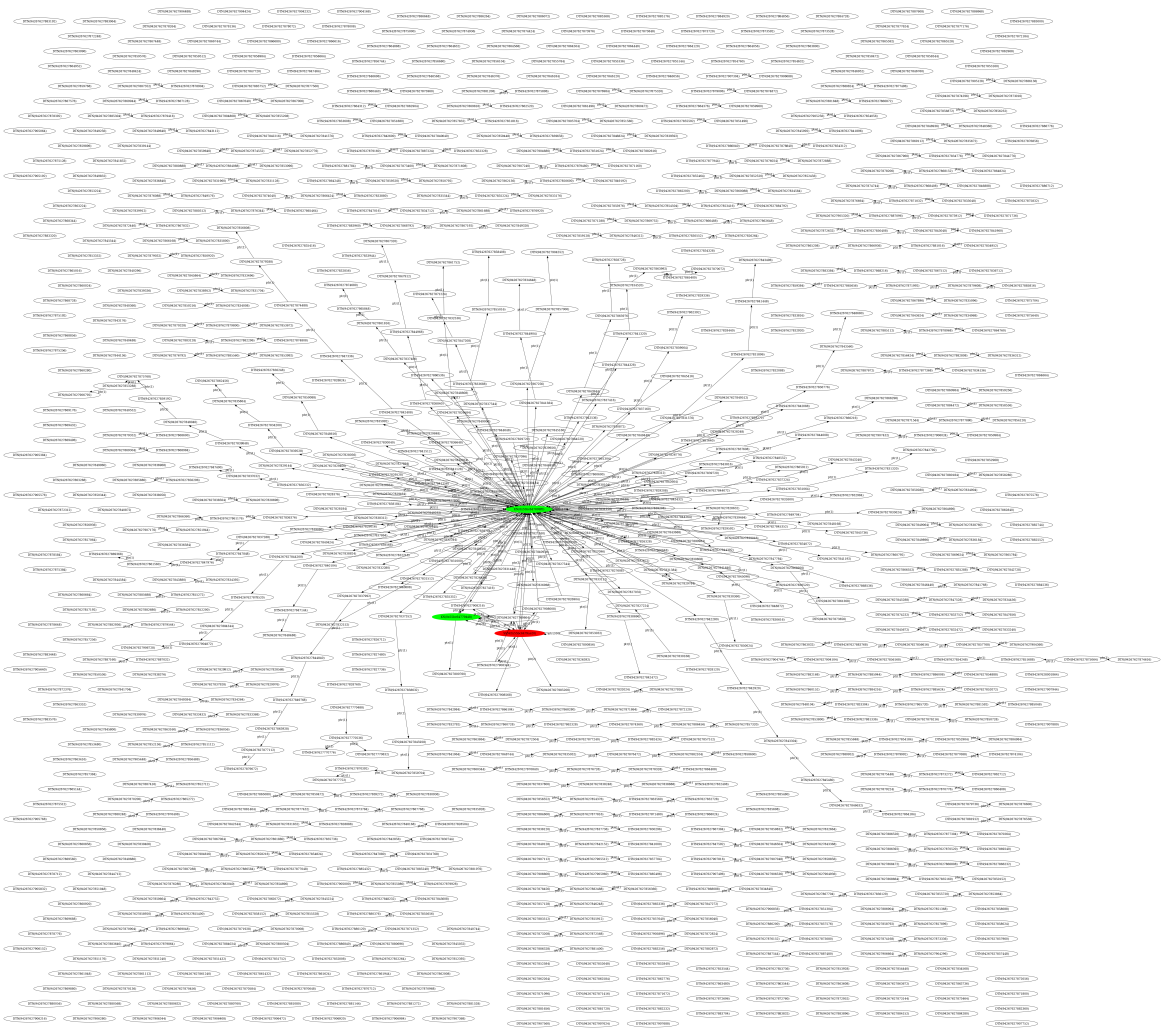

Figure 6.3: Updated graph

6.3 Embedding quality

The quality of embeddings is paramount in machine learning, particularly when the objective is to identify specific chunks within data, such as the ones holding SSH keys. It becomes essential to juxtapose the performances of all embeddings in this context. An optimal embedding should proficiently discern the chunks containing SSH keys across the entire spectrum of openSSH use cases and for every conceivable key size. This necessitates the utilization of the complete dataset, with the training subset dedicated to model training and the validation subset for testing. Addressing this from a machine learning classification perspective, the random forest model, as elucidated in 5.3.4, emerges as the classifier of choice.

To ensure fairness and comparability among the embeddings, we employ the Pearson correlation method 5.3.2.1 to limit the selection to the top 8 correlations, thereby narrowing down our analysis to the most influential features. The dataset is notably imbalanced 5.3.3, primarily stemming from the rarity of memory structures containing SSH keys, our specific target of interest, within the overall dataset. This rarity results in a significant class imbalance, where the majority of memory structures do not contain SSH keys. To counteract potential bias toward the majority class, we will implement random undersampling as a resampling strategy, particularly given our very large dataset. This approach will enable our model to accurately classify both majority and minority classes without being overwhelmed by the sheer volume of data. We will then employ a Random Forest model 5.3, renowned for its robustness and suitability for high-dimensional data, to carry out the classification task. Our evaluation will rely on metrics such as precision, recall, F1 score, and others to identify the most effective representation for precise classification.

6.3.1 Feature Selection and Dataset Challenges

In the quest for fairness across various embeddings and to circumvent the curse of dimensionality, it's imperative to maintain a uniform feature count across all embeddings. This is where feature engineering shines. The Pearson correlation method, elaborated in 5.3.2.1, is harnessed to meticulously select the 8 most salient features for each embedding. This count is a judicious compromise, ensuring the features are both succinct in number and information-rich. However, the dataset presents its own set of challenges. The instances of chunks containing SSH keys are dwarfed by those devoid of them, leading to a pronounced dataset imbalance. To counteract this skewness, the random undersampling technique, as referenced in 5.3.3, is employed.

6.3.2 Implementation and Evaluation Metrics

The implementation leans heavily on the scikit-learn library [26] in Python, which provides the tools for the random forest classifier, Pearson correlation, and the random undersampling algorithm. Concurrently, the pandas library is indispensable for the efficient loading and manipulation of the dataset. Before diving into the analysis, it's crucial to ensure the embedding's integrity. This involves a rigorous sanity check, especially given the potential for corruption, such as NaN values. To guarantee

the reproducibility of results, a consistent random seed is employed for both the random forest classifier and the random undersampling algorithm. For a comprehensive evaluation, the Pearson correlation matrix is preserved for each embedding. Moreover, a suite of metrics, including precision, recall, f1-score, AUC, and the confusion matrix (encompassing true positives, true negatives, false positives, and false negatives), is meticulously saved for every embedding.

7 Results

Describe the experimental setup, the used datasets/parameters and the experimental results achieved

8 Discussion

Discuss the results. What is the outcome of your experimetns?

9 Conclusion

Summarize the thesis and provide a outlook on future work.

10 Ressources

TODO : make transition

10.1 hardware

My primary workstation is an *Aspire 5* laptop, equipped with:

- **CPU:** 11th Gen Intel i5-1135G7 (8) @ 4.200GHz
- **GPU:** Intel TigerLake-LP GT2 [Iris Xe Graphics]
- **Memory:** 16GB

However, this laptop, despite its decent specifications, proved inadequate for processing the entire dataset. Simple machine learning experiments using a Python script would have stretched over a week. Even when we transitioned to more optimized Rust programs, the processing time exceeded 10 hours. While I managed to run minor tasks and scripts on this laptop, the bulk of the experiments necessitated a more powerful server.

Recognizing this need, I was granted access to a high-performance development server in the later stages of the thesis, around August 2023. The server, an *AS-4124GS-TNR*, boasts the following specifications:

- **CPU:** 2x AMD EPYC 7662 (256) @ 2.000GHz
- **GPU:** NVIDIA Geforce RTX 3090 Ti
- **RAM:** 512GB DDR4 3200MHz

Operating on *Ubuntu 20.04.6 LTS*, this server became the primary platform for the machine learning experiments, given its superior computational capabilities compared to the *Aspire 5* laptop. This invaluable resource was generously provided by the Department of Computer Science at *Universität Passau*, particularly under the guidance of the Chair of Data Science led by Prof. Dr. Michael Granitzer. I extend my sincere appreciation for their unwavering support.

A Code

B Math

C Dataset

C.1 Dataset cleaning results

The empty folder for the training part of the dataset after cleaning are :

- Use case: port-forwarding, OpenSSH version: V_8_0_P1, Key size: 64
- Use case: port-forwarding, OpenSSH version: V_8_0_P1, Key size: 32
- Use case: port-forwarding, OpenSSH version: V_7_8_P1, Key size: 16
- Use case: port-forwarding, OpenSSH version: V_7_8_P1, Key size: 64
- Use case: port-forwarding, OpenSSH version: V_7_8_P1, Key size: 32
- Use case: scp, OpenSSH version: V_8_0_P1, Key size: 64
- Use case: scp, OpenSSH version: V_8_0_P1, Key size: 32
- Use case: scp, OpenSSH version: V_7_8_P1, Key size: 64
- Use case: scp, OpenSSH version: V_7_8_P1, Key size: 32
- Use case: basic, OpenSSH version: V_8_7_P1, Key size: 16
- Use case: basic, OpenSSH version: V_8_7_P1, Key size: 64
- Use case: basic, OpenSSH version: V_8_7_P1, Key size: 32
- Use case: basic, OpenSSH version: V_8_8_P1, Key size: 16
- Use case: basic, OpenSSH version: V_8_8_P1, Key size: 64
- Use case: basic, OpenSSH version: V_8_8_P1, Key size: 32
- Use case: basic, OpenSSH version: V_7_0_P1, Key size: 16
- Use case: basic, OpenSSH version: V_7_0_P1, Key size: 64
- Use case: basic, OpenSSH version: V_7_0_P1, Key size: 32
- Use case: basic, OpenSSH version: V_6_8_P1, Key size: 16

- Use case: basic, OpenSSH version: V_6_8_P1, Key size: 64
- Use case: basic, OpenSSH version: V_6_8_P1, Key size: 32
- Use case: basic, OpenSSH version: V_6_2_P1, Key size: 16
- Use case: basic, OpenSSH version: V_6_2_P1, Key size: 24
- Use case: basic, OpenSSH version: V_6_2_P1, Key size: 32
- Use case: basic, OpenSSH version: V_6_0_P1, Key size: 16
- Use case: basic, OpenSSH version: V_6_0_P1, Key size: 24
- Use case: basic, OpenSSH version: V_6_0_P1, Key size: 32
- Use case: basic, OpenSSH version: V_8_1_P1, Key size: 16
- Use case: basic, OpenSSH version: V_8_1_P1, Key size: 64
- Use case: basic, OpenSSH version: V_8_1_P1, Key size: 32
- Use case: basic, OpenSSH version: V_6_1_P1, Key size: 16
- Use case: basic, OpenSSH version: V_6_1_P1, Key size: 24
- Use case: basic, OpenSSH version: V_6_1_P1, Key size: 32
- Use case: basic, OpenSSH version: V_7_2_P1, Key size: 16
- Use case: basic, OpenSSH version: V_7_2_P1, Key size: 64
- Use case: basic, OpenSSH version: V_7_2_P1, Key size: 32
- Use case: basic, OpenSSH version: V_8_0_P1, Key size: 16
- Use case: basic, OpenSSH version: V_8_0_P1, Key size: 64
- Use case: basic, OpenSSH version: V_8_0_P1, Key size: 32
- Use case: basic, OpenSSH version: V_6_3_P1, Key size: 16
- Use case: basic, OpenSSH version: V_6_3_P1, Key size: 24
- Use case: basic, OpenSSH version: V_6_3_P1, Key size: 32
- Use case: basic, OpenSSH version: V_6_9_P1, Key size: 16
- Use case: basic, OpenSSH version: V_6_9_P1, Key size: 64
- Use case: basic, OpenSSH version: V_6_9_P1, Key size: 32
- Use case: basic, OpenSSH version: V_7_1_P1, Key size: 16
- Use case: basic, OpenSSH version: V_7_1_P1, Key size: 64
- Use case: basic, OpenSSH version: V_7_1_P1, Key size: 32

- Use case: basic, OpenSSH version: V_7_9_P1, Key size: 16
- Use case: basic, OpenSSH version: V_7_9_P1, Key size: 64
- Use case: basic, OpenSSH version: V_7_9_P1, Key size: 32
- Use case: basic, OpenSSH version: V_6_7_P1, Key size: 16
- Use case: basic, OpenSSH version: V_6_7_P1, Key size: 24
- Use case: basic, OpenSSH version: V_6_7_P1, Key size: 32
- Use case: basic, OpenSSH version: V_7_8_P1, Key size: 16
- Use case: basic, OpenSSH version: V_7_8_P1, Key size: 64
- Use case: basic, OpenSSH version: V_7_8_P1, Key size: 32
- Use case: client, OpenSSH version: V_8_0_P1, Key size: 16
- Use case: client, OpenSSH version: V_8_0_P1, Key size: 64
- Use case: client, OpenSSH version: V_8_0_P1, Key size: 32
- Use case: client, OpenSSH version: V_7_8_P1, Key size: 16
- Use case: client, OpenSSH version: V_7_8_P1, Key size: 64
- Use case: client, OpenSSH version: V_7_8_P1, Key size: 32

The empty folder for the validation part of the dataset after cleaning are :

- Use case: port-forwarding, OpenSSH version: V_8_0_P1, Key size: 64
- Use case: port-forwarding, OpenSSH version: V_8_0_P1, Key size: 32
- Use case: port-forwarding, OpenSSH version: V_7_8_P1, Key size: 16
- Use case: port-forwarding, OpenSSH version: V_7_8_P1, Key size: 64
- Use case: port-forwarding, OpenSSH version: V_7_8_P1, Key size: 32
- Use case: scp, OpenSSH version: V_8_0_P1, Key size: 64
- Use case: scp, OpenSSH version: V_8_0_P1, Key size: 32
- Use case: scp, OpenSSH version: V_7_8_P1, Key size: 64
- Use case: scp, OpenSSH version: V_7_8_P1, Key size: 32
- Use case: basic, OpenSSH version: V_8_7_P1, Key size: 16
- Use case: basic, OpenSSH version: V_8_7_P1, Key size: 64
- Use case: basic, OpenSSH version: V_8_7_P1, Key size: 32

- Use case: basic, OpenSSH version: V_8_8_P1, Key size: 16
- Use case: basic, OpenSSH version: V_8_8_P1, Key size: 64
- Use case: basic, OpenSSH version: V_8_8_P1, Key size: 32
- Use case: basic, OpenSSH version: V_7_0_P1, Key size: 16
- Use case: basic, OpenSSH version: V_7_0_P1, Key size: 64
- Use case: basic, OpenSSH version: V_7_0_P1, Key size: 32
- Use case: basic, OpenSSH version: V_6_8_P1, Key size: 16
- Use case: basic, OpenSSH version: V_6_8_P1, Key size: 64
- Use case: basic, OpenSSH version: V_6_8_P1, Key size: 32
- Use case: basic, OpenSSH version: V_6_2_P1, Key size: 16
- Use case: basic, OpenSSH version: V_6_2_P1, Key size: 24
- Use case: basic, OpenSSH version: V_6_2_P1, Key size: 32
- Use case: basic, OpenSSH version: V_6_0_P1, Key size: 16
- Use case: basic, OpenSSH version: V_6_0_P1, Key size: 24
- Use case: basic, OpenSSH version: V_6_0_P1, Key size: 32
- Use case: basic, OpenSSH version: V_8_1_P1, Key size: 16
- Use case: basic, OpenSSH version: V_8_1_P1, Key size: 64
- Use case: basic, OpenSSH version: V_8_1_P1, Key size: 32
- Use case: basic, OpenSSH version: V_6_1_P1, Key size: 16
- Use case: basic, OpenSSH version: V_6_1_P1, Key size: 24
- Use case: basic, OpenSSH version: V_6_1_P1, Key size: 32
- Use case: basic, OpenSSH version: V_7_2_P1, Key size: 16
- Use case: basic, OpenSSH version: V_7_2_P1, Key size: 64
- Use case: basic, OpenSSH version: V_7_2_P1, Key size: 32
- Use case: basic, OpenSSH version: V_8_0_P1, Key size: 16
- Use case: basic, OpenSSH version: V_8_0_P1, Key size: 64
- Use case: basic, OpenSSH version: V_8_0_P1, Key size: 32
- Use case: basic, OpenSSH version: V_6_3_P1, Key size: 16
- Use case: basic, OpenSSH version: V_6_3_P1, Key size: 24

- Use case: basic, OpenSSH version: V_6_3_P1, Key size: 32
- Use case: basic, OpenSSH version: V_6_9_P1, Key size: 16
- Use case: basic, OpenSSH version: V_6_9_P1, Key size: 64
- Use case: basic, OpenSSH version: V_6_9_P1, Key size: 32
- Use case: basic, OpenSSH version: V_7_1_P1, Key size: 16
- Use case: basic, OpenSSH version: V_7_1_P1, Key size: 64
- Use case: basic, OpenSSH version: V_7_1_P1, Key size: 32
- Use case: basic, OpenSSH version: V_7_9_P1, Key size: 16
- Use case: basic, OpenSSH version: V_7_9_P1, Key size: 64
- Use case: basic, OpenSSH version: V_7_9_P1, Key size: 32
- Use case: basic, OpenSSH version: V_6_7_P1, Key size: 16
- Use case: basic, OpenSSH version: V_6_7_P1, Key size: 24
- Use case: basic, OpenSSH version: V_6_7_P1, Key size: 32
- Use case: basic, OpenSSH version: V_7_8_P1, Key size: 16
- Use case: basic, OpenSSH version: V_7_8_P1, Key size: 64
- Use case: basic, OpenSSH version: V_7_8_P1, Key size: 32
- Use case: client, OpenSSH version: V_8_0_P1, Key size: 16
- Use case: client, OpenSSH version: V_8_0_P1, Key size: 64
- Use case: client, OpenSSH version: V_8_0_P1, Key size: 32
- Use case: client, OpenSSH version: V_7_8_P1, Key size: 16
- Use case: client, OpenSSH version: V_7_8_P1, Key size: 32

Acronyms

BFD Byte Frequency Distribution. 5–7

CNN Convolutional Neural Networks. 5, 8, 10, 11

GRU Gated Recurrent Units. 5, 9

KNN K-Nearest Neighbors. 17

LSB Least Significant Bit. 25

LSTM Long Short-Term Memory. 5, 9, 10

OPTICS Ordering Points To Identify the Clustering Structure. 19–21

PCA Principal Component Analysis. 15

RCNN Recurrent Convolutional Neural Network. 8

REGEX regular expressions. 35

RNN Recurrent Neural Networks. 5, 8–10

Seq2Seq Sequence-to-Sequence. 10, 11

SMOTE Synthetic Minority Over-sampling Technique. 16

SSH Secure Shell. 1

SVM Support Vector Machines. 17

t-SNE t-Distributed Stochastic Neighbor Embedding. 15

VMI Virtual Machine Introspection. 1, 2

Glossary

chunk In our study, chunks are defined as a series of bytes that are allocated in the heap. These structures are allocated using the `malloc` function and begin everytime by a *malloc header*. v, 24–27

pointer In our study, pointers are characterized as sequences of hexadecimal numbers that reference distinct memory addresses. These sequences can be recognized using the following regular expression: `"[0-9a-f]{12}0{4}"`. 31, 34–37

. 31, 34–37, 39

value node In our study, value nodes represent 8-byte blocks of data that are contained within a structure.. 35, 36

References

[1] Mihael Ankerst et al. „OPTICS: Ordering Points To Identify the Clustering Structure“. In: *ACM SIGMOD Record* 28 (June 1999), pp. 49–60. DOI: 10.1145/304181.304187.

[2] Shaojie Bai, J. Zico Kolter, and Vladlen Koltun. *An Empirical Evaluation of Generic Convolutional and Recurrent Networks for Sequence Modeling*. Apr. 19, 2018. arXiv: 1803.01271[cs]. URL: http://arxiv.org/abs/1803.01271 (visited on 08/23/2023).

[3] Richard Boddy and Gordon Smith. *Statistical methods in practice: for scientists and technologists*. John Wiley & Sons, 2009.

[4] Meghan K. Cain, Zhiyong Zhang, and Ke-Hai Yuan. „Univariate and multivariate skewness and kurtosis for measuring nonnormality: Prevalence, influence and estimation“. In: *Behavior Research Methods* 49.5 (Oct. 2017), pp. 1716–1735. ISSN: 1554-3528. DOI: 10.3758/s13428-016-0814-1. URL: http://link.springer.com/10.3758/s13428-016-0814-1 (visited on 08/30/2023).

[5] Junyoung Chung et al. *Empirical Evaluation of Gated Recurrent Neural Networks on Sequence Modeling*. Dec. 11, 2014. arXiv: 1412.3555[cs]. URL: http://arxiv.org/abs/1412.3555 (visited on 08/23/2023).

[6] D. J. Delorie et al. *Malloc Internals*. Publisher: Sourceware. 2023. URL: https://sourceware.org/glibc/wiki/MallocInternals (visited on 09/25/2023).

[7] John Ellson et al. „Graphviz and Dynagraph — Static and Dynamic Graph Drawing Tools“. In: *Graph Drawing Software*. Ed. by Michael Jünger and Petra Mutzel. Red. by Gerald Farin et al. Series Title: Mathematics and Visualization. Berlin, Heidelberg: Springer Berlin Heidelberg, 2004, pp. 127–148. ISBN: 978-3-642-62214-4 978-3-642-18638-7. DOI: 10.1007/978-3-642-18638-7_6. URL: http://link.springer.com/10.1007/978-3-642-18638-7_6 (visited on 09/11/2023).

[8] Martin Ester et al. „A Density-Based Algorithm for Discovering Clusters in Large Spatial Databases with Noise“. In: *KDD-96* (Aug. 2, 1996).

[9] Christofer Fellicious et al. *SmartKex: Machine Learning Assisted SSH Keys Extraction From The Heap Dump*. Sept. 13, 2022. arXiv: 2209.05243[cs]. URL: http://arxiv.org/abs/2209.05243 (visited on 08/17/2023).

[10] Jonas Gehring et al. „Convolutional Sequence to Sequence Learning“. In: *Facebook AI Research* (July 25, 2017). URL: https://arxiv.org/pdf/1705.03122.pdf.

[11] Wolfram Gloger and Doug Lea. *Malloc implementation for multiple threads without lock contention*. Publisher: Free Software Foundation, Inc. 2001. URL: https://elixir.bootlin.com/glibc/glibc-2.28/source/malloc/malloc.c (visited on 09/22/2023).

[12] Luke Hiester. „File Fragment Classification Using Neural Networks with Lossless Representations“. In: *East Tennessee State University* (May 2018). (Visited on 08/21/2023).

[13] G. E. Hinton and R. R. Salakhutdinov. „Reducing the Dimensionality of Data with Neural Networks“. In: *Science* 313.5786 (July 28, 2006), pp. 504–507. ISSN: 0036-8075, 1095-9203. DOI: 10.1126/science.1127647. URL: https://www.science.org/doi/10.1126/science.1127647 (visited on 08/30/2023).

[14] Sepp Hochreiter and Jürgen Schmidhuber. „Long short-term memory“. In: *Neural computation* 9.8 (1997). Publisher: MIT Press, pp. 1735–1780. (Visited on 08/23/2023).

[15] Samina Khalid, Tehmina Khalil, and Shamila Nasreen. „A survey of feature selection and feature extraction techniques in machine learning“. In: *2014 Science and Information Conference*. 2014 Science and Information Conference. Aug. 2014, pp. 372–378. DOI: 10.1109/SAI.2014.6918213.

[16] Udayan Khurana, Horst Samulowitz, and Deepak Turaga. *Feature Engineering for Predictive Modeling using Reinforcement Learning*. Sept. 21, 2017. arXiv: 1709.07150[cs,stat]. URL: http://arxiv.org/abs/1709.07150 (visited on 08/30/2023).

[17] Mario Koppen. „The curse of dimensionality“. In: 1 (2000), pp. 4–8.

[18] S. B. Kotsiantis. „Decision trees: a recent overview“. In: *Artificial Intelligence Review* 39.4 (Apr. 2013), pp. 261–283. ISSN: 0269-2821, 1573-7462. DOI: 10.1007/s10462-011-9272-4. URL: http://link.springer.com/10.1007/s10462-011-9272-4 (visited on 08/30/2023).

[19] J. Laaksonen and E. Oja. „Classification with learning k-nearest neighbors“. In: *Proceedings of International Conference on Neural Networks (ICNN'96)*. International Conference on Neural Networks (ICNN'96). Vol. 3. Washington, DC, USA: IEEE, 1996, pp. 1480–1483. ISBN: 978-0-7803-3210-2. DOI: 10.1109/ICNN.1996.549118. URL: http://ieeexplore.ieee.org/document/549118/ (visited on 08/30/2023).

[20] Siwei Lai et al. „Recurrent Convolutional Neural Networks for Text Classification“. In: *Proceedings of the AAAI Conference on Artificial Intelligence* 29.1 (Feb. 19, 2015). ISSN: 2374-3468, 2159-5399. DOI: 10.1609/aaai.v29i1.9513. URL: https://ojs.aaai.org/index.php/AAAI/article/view/9513 (visited on 08/23/2023).

[21] Yann LeCun et al. „Gradient-Based Learning Applied to Document Recognition“. In: *proc of the IEEE* (1998).

[22] Ulrike von Luxburg. *A Tutorial on Spectral Clustering*. Nov. 1, 2007. arXiv: 0711.0189[cs]. URL: http://arxiv.org/abs/0711.0189 (visited on 09/05/2023).

[23] J Macqueen. „SOME METHODS FOR CLASSIFICATION AND ANALYSIS OF MULTIVARIATE OBSERVATIONS“. In: *MULTIVARIATE OBSERVATIONS* VOL. 5.1 (1967).

[24] Tomas Mikolov et al. *Efficient Estimation of Word Representations in Vector Space*. Sept. 6, 2013. arXiv: 1301.3781[cs]. URL: http://arxiv.org/abs/1301.3781 (visited on 10/18/2023).

[25] Todd G Nick and Kathleen M Campbell. „Logistic regression“. In: *Topics in biostatistics* (2007). Publisher: Springer, pp. 273–301.

[26] F. Pedregosa et al. „Scikit-learn: Machine Learning in Python“. In: *Journal of Machine Learning Research* 12 (2011), pp. 2825–2830.

[27] Philipp Probst, Marvin Wright, and Anne-Laure Boulesteix. „Hyperparameters and Tuning Strategies for Random Forest“. In: *WIREs Data Mining and Knowledge Discovery* 9.3 (May 2019), e1301. ISSN: 1942-4787, 1942-4795. DOI: 10.1002/widm.1301. arXiv: 1804.03515[cs,stat]. URL: http://arxiv.org/abs/1804.03515 (visited on 08/30/2023).

[28] Dr D Ramyachitra and P Manikandan. „IMBALANCED DATASET CLASSIFICATION AND SOLUTIONS: A REVIEW“. In: *International Journal of Computing and Business Research* 5.4 (2014).

[29] Stewart Sentanoe and Hans P. Reiser. „SSHkex: Leveraging virtual machine introspection for extracting SSH keys and decrypting SSH network traffic“. In: *Forensic Science International: Digital Investigation* 40 (Apr. 2022), p. 301337. ISSN: 26662817. DOI: 10.1016/j.fsidi.2022.301337. URL: https://linkinghub.elsevier.com/retrieve/pii/S2666281722000063 (visited on 08/17/2023).

[30] C E Shannon. „A Mathematical Theory of Communication“. In: *The Bell System Technical Journa* 27 (Oct. 1948), pp. 379–423.

[31] Ilya Sutskever, Oriol Vinyals, and Quoc V. Le. *Sequence to Sequence Learning with Neural Networks*. Dec. 14, 2014. arXiv: 1409.3215[cs]. URL: http://arxiv.org/abs/1409.3215 (visited on 08/23/2023).

[32] Unknown. *How does glibc malloc work?* 2023. URL: https://reverseengineering.stackexchange.com/questions/15033/how-does-glibc-malloc-work/15038#15038.

[33] Ashish Vaswani et al. „Attention Is All You Need“. In: *Advances in Neural Information Processing Systems* 30 (2017), pp. 5998–6008. (Visited on 08/23/2023).

[34] Michel Verleysen and Damien François. „The Curse of Dimensionality in Data Mining and Time Series Prediction“. In: *Computational Intelligence and Bioinspired Systems*. Ed. by Joan Cabestany, Alberto Prieto, and Francisco Sandoval. Red. by David Hutchison et al. Vol. 3512. Series Title: Lecture Notes in Computer Science. Berlin, Heidelberg: Springer Berlin Heidelberg, 2005, pp. 758–770. ISBN: 978-3-540-26208-4 978-3-540-32106-4. DOI: 10.1007/11494669_93. URL: http://link.springer.com/10.1007/11494669_93 (visited on 08/30/2023).

[35] Donald J Wheeler. „Problems with Skewness and Kurtosis“. In: *Quality Digest Daily* (Aug. 1, 2011).

[36] Qiang Wu and Ding-Xuan Zhou. „Analysis of Support Vector Machine Classification“. In: *Journal of Computational Analysis & Applications* 8.2 (2006).

Additional bibliography

[37] Walter T. Ambrosius, ed. *Topics in biostatistics*. Methods in molecular biology 404. OCLC: ocn159977868. Totowa, N.J: Humana Press, 2007. 528 pp. ISBN: 978-1-58829-531-6.

[38] *CERT/CC Vulnerability Note VU#13877*. URL: https://www.kb.cert.org (visited on 08/30/2023).

[39] Vic Degraeve et al. „R-GCN: the R could stand for random“. In: *arXiv:2203.02424 preprint* (2022). URL: https://arxiv.org/pdf/2203.02424.pdf.

[40] Christofer Fellicious et al. *Machine Learning Assisted SSH Keys Extraction From The Heap Dump*. Version 0.1. Aug. 15, 2022. DOI: 10.5281/ZENODO.6537904. URL: https://zenodo.org/record/6537904 (visited on 09/06/2023).

[41] Vivek Gite. *How To Reuse SSH Connection To Speed Up Remote Login Process Using Multiplexing*. nixCraft. Aug. 20, 2008. URL: https://www.cyberciti.biz/faq/linux-unix-reuse-openssh-connection/ (visited on 10/21/2022).

[42] Jose Manuel Gomez-Perez, Ronald Denaux, and Andres Garcia-Silva. „Understanding Word Embeddings and Language Models“. In: *A Practical Guide to Hybrid Natural Language Processing: Combining Neural Models and Knowledge Graphs for NLP*. Ed. by Jose Manuel Gomez-Perez, Ronald Denaux, and Andres Garcia-Silva. Cham: Springer International Publishing, 2020, pp. 17–31. ISBN: 978-3-030-44830-1. DOI: 10.1007/978-3-030-44830-1_3. URL: https://doi.org/10.1007/978-3-030-44830-1_3 (visited on 09/08/2023).

[43] Ian Goodfellow, Yoshua Bengio, and Aaron Courville. *Deep learning*. MIT press, 2016. URL: https://books.google.de/books?hl=en&lr=&id=omivDQAAQBAJ&oi=fnd&pg=PR5&dq=deep+learning&ots=MNV2eosBRS&sig=jN2QwFikq3g_YqU3hJVPEP0XIJ4&redir_esc=y#v=onepage&q=deep%20learning&f=false.

[44] Aidan Hogan et al. „Knowledge Graphs (Extended)“. In: *ACM Computing Surveys* 54.4 (May 31, 2022), pp. 1–37. ISSN: 0360-0300, 1557-7341. DOI: 10.1145/3447772. arXiv: 2003.02320[cs]. URL: http://arxiv.org/abs/2003.02320 (visited on 09/08/2023).

[45] Weijie Huang and Jun Wang. *Character-level Convolutional Network for Text Classification Applied to Chinese Corpus*. Nov. 15, 2016. arXiv: 1611.04358[cs]. URL: http://arxiv.org/abs/1611.04358 (visited on 08/17/2023).

[46] Michael I Jordan and Tom M Mitchell. „Machine learning: Trends, perspectives, and prospects“. In: *Science* 349.6245 (2015). Publisher: American Association for the Advancement of Science, pp. 255–260. URL: https://www.science.org/doi/full/10.1126/science.aaa8415.

[47] Ye Liu et al. „Kg-bart: Knowledge graph-augmented bart for generative commonsense reasoning“. In: *Proceedings of the AAAI Conference on Artificial Intelligence*. Vol. 35. Issue: 7. 2021, pp. 6418–6425. URL: file:///home/onyr/Downloads/16796-Article%20Text-20290-1-2-20210518.pdf.

[48] José Tomás Martínez Garre, Manuel Gil Pérez, and Antonio Ruiz-Martínez. „A novel Machine Learning-based approach for the detection of SSH botnet infection“. In: *Future Generation Computer Systems* 115 (Feb. 1, 2021), pp. 387–396. ISSN: 0167-739X. DOI: 10.1016/j.future.2020.09.004. URL: https://www.sciencedirect.com/science/article/pii/S0167739X20303265 (visited on 08/30/2023).

[49] Dai Quoc Nguyen et al. „A Novel Embedding Model for Knowledge Base Completion Based on Convolutional Neural Network“. In: *Proceedings of the 2018 Conference of the North American Chapter of the Association for Computational Linguistics: Human Language Technologies, Volume 2 (Short Papers)*. Association for Computational Linguistics, 2018. DOI: 10.18653/v1/n18-2053. URL: https://doi.org/10.18653%2Fv1%2Fn18-2053.

[50] Michael Schlichtkrull et al. „Modeling relational data with graph convolutional networks“. In: *The Semantic Web: 15th International Conference, ESWC 2018, Heraklion, Crete, Greece, June 3–7, 2018, Proceedings 15*. Springer, 2018, pp. 593–607. URL: https://arxiv.org/pdf/1703.06103.pdf.

[51] Daixin Wang, Peng Cui, and Wenwu Zhu. „Structural Deep Network Embedding“. In: *Proceedings of the 22nd ACM SIGKDD International Conference on Knowledge Discovery and Data Mining*. KDD '16: The 22nd ACM SIGKDD International Conference on Knowledge Discovery and Data Mining. San Francisco California USA: ACM, Aug. 13, 2016, pp. 1225–1234. ISBN: 978-1-4503-

4232-2. DOI: 10.1145/2939672.2939753. URL: https://dl.acm.org/doi/10.1145/2939672.2939753 (visited on 09/11/2023).

[52] Liang Yao, Chengsheng Mao, and Yuan Luo. „KG-BERT: BERT for knowledge graph completion“. In: *arXiv preprint arXiv:1909.03193* (2019). URL: https://arxiv.org/pdf/1909.03193.pdf.

[53] W. Yurcik and Chao Liu. „A first step toward detecting SSH identity theft in HPC cluster environments: discriminating masqueraders based on command behavior“. In: *CCGrid 2005. IEEE International Symposium on Cluster Computing and the Grid, 2005.* CCGrid 2005. IEEE International Symposium on Cluster Computing and the Grid, 2005. Vol. 1. May 2005, 111–120 Vol. 1. DOI: 10.1109/CCGRID.2005.1558542.

[54] Jianlong Zhou et al. „Evaluating the Quality of Machine Learning Explanations: A Survey on Methods and Metrics“. In: *Electronics* 10.5 (Mar. 4, 2021), p. 593. ISSN: 2079-9292. DOI: 10.3390/electronics10050593. URL: https://www.mdpi.com/2079-9292/10/5/593 (visited on 09/11/2023).

Eidesstattliche Erklärung

Hiermit versichere ich, dass ich diese Masterarbeit selbstständig und ohne Benutzung anderer als der angegebenen Quellen und Hilfsmittel angefertigt habe und alle Ausführungen, die wörtlich oder sinngemäß übernommen wurden, als solche gekennzeichnet sind, sowie, dass ich die Masterarbeit in gleicher oder ähnlicher Form noch keiner anderen Prüfungsbehörde vorgelegt habe.

Passau, October 18, 2023

_____

Lahoche, Clément Claude Martial